

SKYSCENES: A Synthetic Dataset for Aerial Scene Understanding

Sahil Khose*

Anisha Pal*¹Aayushi Agarwal*¹Deepanshi*¹Judy Hoffman¹Prithvijit Chattopadhyay¹

Georgia Institute of Technology

{sahil.khose, apal72, judy, prithvijit3}@gatech.edu

{aayushi.agarwal007, deepanshi.asr.21}@gmail.com

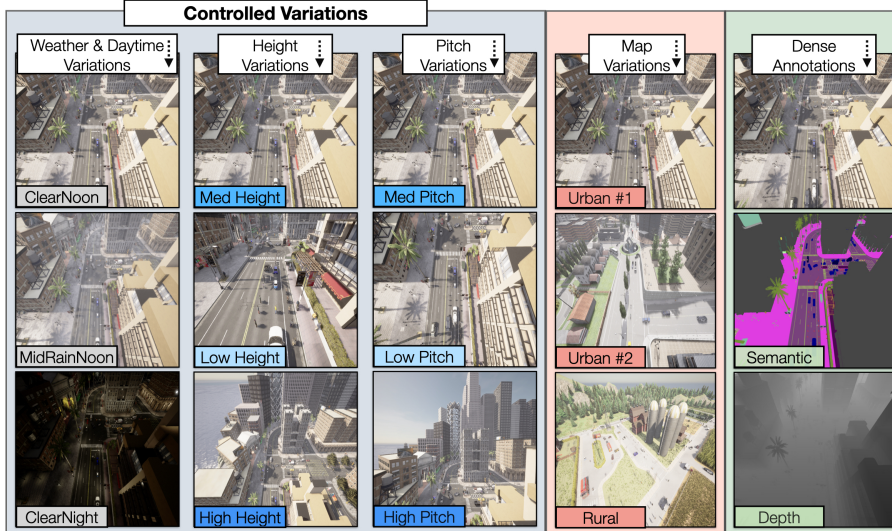
<https://huggingface.co/datasets/hoffman-lab/SkyScenes>

Fig. 1: SKYSCENES comprises of 33.6k aerial images curated from aerial oblique viewpoints with **controlled variations** facilitating reproducibility of viewpoints across different weather and daytime conditions (col 1), different flying altitudes (col 2) and different viewpoint pitch angles (col 3), across different map layouts (rural and urban, col 4) with dense pixel-level semantic, instance and depth annotations (col 5).

Abstract. Real-world aerial scene understanding is limited by a lack of datasets that contain densely annotated images curated under a diverse set of conditions. Due to inherent challenges in obtaining such images in controlled real-world settings, we present SKYSCENES, a synthetic

* Equal Contribution

The 18th European Conference on Computer Vision ECCV 2024

dataset of densely annotated aerial images captured from Unmanned Aerial Vehicle (UAV) perspectives. We carefully curate SKYSCENES images from CARLA to comprehensively capture diversity across layouts (urban and rural maps), weather conditions, times of day, pitch angles and altitudes with corresponding semantic, instance and depth annotations. Through our experiments using SKYSCENES, we show that (1) models trained on SKYSCENES generalize well to different real-world scenarios, (2) augmenting training on real images with SKYSCENES data can improve real-world performance, (3) controlled variations in SKYSCENES can offer insights into how models respond to changes in viewpoint conditions (height and pitch), weather and time of day, and (4) incorporating additional sensor modalities (depth) can improve aerial scene understanding. Our dataset and associated generation code are publicly available at: <https://hoffman-group.github.io/SkyScenes/>

Keywords: Aerial scene understanding, Synthetic-to-Real generalization, Segmentation, Domain Generalization, Synthetic Data

1 Introduction

Aerial imagery provides a unique perspective that is invaluable for a wide range of applications, including surveillance [33, 39], mapping [3, 37], urban planning [13, 24], environmental monitoring [7, 29], and disaster response [21, 31]. These applications rely on accurate and detailed analysis of aerial images to make informed decisions and effectively address various challenges. Naturally, training effective aerial scene-understanding models requires access to large-scale annotated exemplar data that have been *carefully curated* under diverse conditions. Capturing such images not only allows training models that can be robust to anticipated test-time variations but also allows assessing model susceptibility to changing conditions. However, carefully curating and annotating such images in the real-world can be prohibitively expensive due to various reasons. First, densely annotating every pixel of high-resolution real-world aerial images is expensive – for instance, densely annotating a single 4K image in UAVid [27] can take up to 2 hours! Second, although diversity in training data is vital for developing robust generalization algorithms and for model sensitivity assessment, expanding the real set to include widespread variations (weather, time of day, pitch, altitude) would be uncontrolled (*i.e.*, we can't guarantee the same viewpoint under different conditions as the real world is not static), and hence would require re-annotating newly captured frames. Synthetic data curated from simulators can help counter both these issues as (1) labels are automatic and cheap to obtain and (2) it is possible to recreate same viewpoint (with same scene layout and actor instances, `vehicles`, `humans`, etc. in the scene) under differing conditions.

The unique challenges introduced by outdoor aerial imagery setting such as variability in altitude and angle of image capture, skewed representation for classes with smaller object sizes (`humans`, `vehicles`), size and occlusion variations of

object classes in the same image, etc., make it a relatively difficult problem compared to ground-view imagery setting. This is illustrated by the observation that the current developments in syn-to-real generalization methods [16, 54] have resulted in a significant reduction in the syn-to-real generalization gap in ground-view settings to as minimal as 20%¹, compared to the comparatively higher margin observed in aerial imagery scenarios, reaching up to 50% (see Sec. D.3, D.4, D.5 in appendix). Unlike synthetic ground plane view datasets (especially for autonomous driving [8, 32, 43, 46, 56]), synthetic datasets for aerial imagery (see Table. 1, rows 4-10) have received relatively less attention [5, 12, 23, 25, 42, 47, 53]. While existing synthetic aerial imagery datasets have tried to close this gap, they are often found lacking in a few different aspects – complementary metadata to reproduce existing frame viewpoints under different conditions, limited diversity, availability of dense annotations for a wide vocabulary of classes and image capture (height, pitch) conditions (see Table. 1 for an exhaustive summary). These synthetic aerial datasets rarely allow for reproducing the exact viewpoint with different variations based on detailed scene metadata (see Table. 1 Controlled Variations column), a key aspect for evaluating deep learning models’ responses to changing conditions and assessing sensitivity to single-variable alterations (e.g., weather, time of day, sensor angle).

We cover all these aspects by introducing SKYSCENES, a synthetic dataset containing 33.6k densely annotated aerial scenes, leveraging the CARLA [10] simulator to capture diverse *layout* (urban and rural), *weather*, *daytime*, *pitch* and *altitude* conditions. Our pipeline meticulously generates scenes with precise actor locations and orientations, ensuring each scene’s reproducibility with a comprehensive metadata store and rigorous consistency checks.

SKYSCENES encompasses detailed semantic, instance segmentation (28 classes), and depth annotations across 8 distinct map layouts across 5 different weather and daytime conditions each over a combination of 3 altitude and 4 pitch variations (see Fig. 1 for examples). While doing so, we keep several important desiderata in mind. First, we ensure that stored snapshots are not correlated, to promote diverse viewpoints within a town and facilitate model training. Second, we store all metadata associated with the position of actors, camera, and other scene elements to be able to reproduce the same viewpoints under different weather and daytime conditions. Thirdly, we ensure that the generated data mimics real-world imperfections by introducing variations in sensor locations, such as adding jitter to specified height and pitch values.² Finally, since CARLA [10] by default does not spawn a lot of pedestrians in a scene, we propose an algorithm to ensure adequate representation of **humans** in the scene while curating images (see Sec. 3.1 and Sec. 3.2 for a detailed discussion).

Our experiments across 3 different real datasets and 3 increasingly competitive semantic segmentation architectures consistently demonstrate that SKYSCENES outperforms its closest synthetic counterpart dataset, SYNDRONE [42]. However,

¹ metric of choice: mIoU.

² Moreover, through rigorous validations, we ensure this process is consistent and yields error-free re-generations. See Sec. 3.1.

despite these dataset-level improvements, the syn-to-real generalization gap persists, indicating that algorithmic improvements developed for ground-view imagery fail to translate effectively to aerial imagery. This underscores the urgent need for specialized algorithmic development in this area.

Empirically, we demonstrate the utility of SKYSCENES in several different ways. First, we show that SKYSCENES is a valuable pre-training dataset for real-world aerial scene understanding by, (1) demonstrating that models trained on SKYSCENES generalize well to multiple real-world datasets and (2) demonstrating that SKYSCENES pretraining improves real-world performance in low-shot regimes. Second, we show that controlled variations in SKYSCENES can serve as a diagnostic test-bed to assess model sensitivity to weather, daytime, pitch, altitude, and layout conditions – by testing SKYSCENES trained models in unseen SKYSCENES conditions. Finally, we show that SKYSCENES can enable developing multi-modal segmentation models with improved aerial-scene understanding capabilities when additional sensors, such as Depth, are available. To summarize, we make the following contributions:

- We introduce, SKYSCENES, a densely-annotated dataset of 33.6k synthetic aerial images. SKYSCENES contains images from different altitude and pitch settings, encompassing different layouts, weather, and daytime conditions with corresponding dense annotations and viewpoint metadata.
- We demonstrate that SKYSCENES pre-trained models generalize well to real-world scenes and that SKYSCENES data can effectively augment real-world training data for improved performance. We also bring attention to the point that while the synthetic-to-real gap has considerably narrowed for ground-view datasets, the same algorithms are unable to bridge this gap in aerial imagery.
- We show that our unique ability to generate controlled variations enables SKYSCENES to serve as a diagnostic test-bed to assess model sensitivity to changing weather, daytime, pitch, altitude, and layout conditions.
- Finally, we show that incorporating additional modalities (depth) while training aerial scene-understanding models can improve aerial scene recognition, enabling further development of multi-modal segmentation models.

2 Related Work

Ground-view Synthetic Datasets. Real-world ground-view scene-understanding datasets (Cityscapes [8], Mapillary [32], BDD-100K [56], Dark Zurich [45]) fail to capture the full range of variations that exist in the world. Synthetic data is a popular alternative for generating diverse and bountiful views. GTAV [46], Synthia [43], and VisDA-C [38] are some of the widely-used synthetic datasets. These datasets can be curated using underlying simulators, such as GTAV [46] game engine and CARLA [10] simulator and offer a cost-effective and scalable way to generate large amounts of labeled data under diverse conditions. Similar to SELMA [50] and SHIFT [49], we use CARLA [10] as the underlying simulator for SKYSCENES.

Dataset	Controlled Variations	Diversity			Annotation Diversity	Altitude	Perspective	Resolution	Scale
		Town	Daytime	Weather					
Real									
1 UAVid [27]	✗	✗	✗	✗	S	Med	Obl.	3840 × 2160	0.42k
2 AeroScapes [34]	✗	✗	✗	✗	S	(Low, Med)	(Obl., Nad.)	1280 × 720	3.27k
3 ICG Drone [20]	✗	✗	✗	✗	S	Low	Nad.	6000 × 4000	0.6k
Synthetic									
4 Espada [25]	✗	✓	✗	✗	D	(Med, High)	Nad.	640 × 480	80k
5 UrbanScene3D [23]	✗	✓	✗	✗	-	Med	Obl.	6000 × 4000	128k
6 SynthAer [47]	✓	✗	✓	✗	S	(Low, Med)	Obl.	1280 × 720	~0.77k
7 MidAir [12]	✗	✓	✓	✓	(S,D)	Low	(Obl., Nad.)	1024 × 1024	119k
8 TartanAir [53]	✗	✓	✓	✓	(S,D)	Low	(Fwd., Obl.)	640 × 480	~1M
9 VALID [5]	✗	✓	✓	✓	(S,I,D)	(Low, Med, High)	Nad.	1024 × 1024	6.7k
10 SynDrone [42]	✗	✓	✗	✗	(S,D)	(Low, Med, High)	(Obl., Nad.)	1920 × 1080	72k
11 SKYSCENES	✓	✓	✓	✓	(S,I,D)	(Low, Med, High)	(Fwd., Obl., Nad.)	2160 × 1440	33.6k

Table 1: SKYSCENES compared with other Real and Synthetic Datasets.

We compare SKYSCENES (row 11) with other real (rows 1 – 3) and synthetic (rows 4 – 10) aerial datasets across several axes: (i) **Controlled Variations** – the ability to reproduce the exact viewpoint under different variations from fine-grained scene metadata, (ii) **Diversity** – diversity of map layouts (rural, urban), weather and daytime conditions in the provided images, (iii) **Annotation Diversity** – supporting dense annotations across depth (D), semantic(S) and instance segmentation (I) tasks, (iv) **Altitude** – altitude of image capture; Low is $< 30\text{m}$, Med is $\in [30, 50]\text{m}$ and High is $> 50\text{m}$, (v) **Perspective** – UAV pitch angle during image capture; Fwd. is forward view with $\theta = 0^\circ$, Obl. is oblique view with $\theta \in (0^\circ, 90^\circ)$ and Nad. is nadir view with $\theta = 90^\circ$ (θ is pitch), (vi) **Resolution** – resolution of the images, (vii) **Scale** – number of images. We see that while existing datasets might be lacking in a subset of criteria, SKYSCENES fulfills all of these.

Real-World Aerial Datasets. To support remote sensing applications, it is crucial to have access to datasets that offer aerial-specific views. Datasets such as GID [51], DeepGlobe [9], ISPRS2D [44], and FloodNet [40] primarily provide nadir perspectives and are designed for scene-recognition and understanding tasks. However, this study specifically focuses on lower altitudes, which are more relevant to UAVs, enabling object identification. Unfortunately, there is a scarcity of high-resolution real-world datasets based on UAV imagery emphasizing object identification. Existing urban scene datasets, like AeroScapes [34], UAVid [27], VDD [1], UDD [6], UAVDT [11], VisDrone [57], Semantic Drones [20] and others, suffer from limited sizes and a lack of diverse images under different conditions. This limitation raises concerns regarding model robustness and generalization.

Synthetic Aerial Datasets. Simulators can facilitate affordable, reliable, and quick collection of large synthetic aerial datasets, which aids in fast prototyping, improves real-world performance by enhancing robustness, and enables controlled studies on varied conditions. One such high-fidelity simulator, AirSim [48], used for development and testing of autonomous systems (in particular, aerial vehicles), is the foundation of several synthetic UAV-based datasets – MidAir [12], Espada [25], Tartan Air [53], UrbanScene3D [23] and VALID [5]. CARLA [10] is another such open-source simulator that is the foundation of datasets like SynDrone [42]. However, these datasets fall short in capturing real-world irregularities, lack deterministic re-generation capabilities, controlled diversity in weather and daytime conditions, and exhibit skewed representation for certain

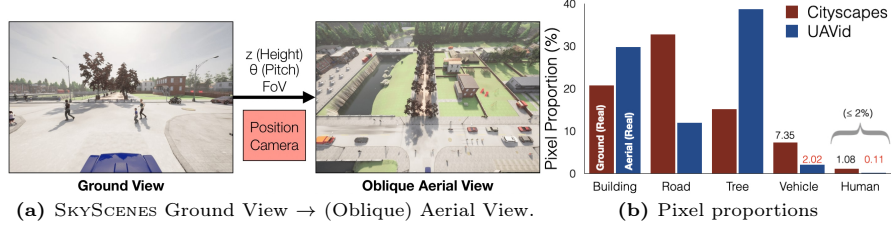


Fig. 2: Ground View → (Oblique) Aerial View. (a) The same scene viewed in Ground View vs Aerial View exhibits a significant difference in pixel proportion especially across the tail classes (**vehicle**, **human**) (b) For a subset of commonly annotated classes across CityScapes [8] (red), UAVid [27] (dark blue), we show the percentage of pixels occupied by different classes. Aerial scenes (in UAVid) have significant under-representation of tail classes (**vehicle**, **human**).

classes (differences summarized in Table. 1). This restricts their ability to generalize well to real-world datasets and their usage as a diagnostic tool for studying the controlled effect of diversity on the performance of computer vision perception tasks. To enable such studies, SKYSCENES offers images featuring varied scenes, diverse weather, daytime, altitude, and pitch variations while incorporating real-world irregularities and addressing skewed class representation along with simultaneous depth, semantic, and instance segmentation annotations.

3 SKYSCENES

We curate SKYSCENES using, CARLA [10]³ 0.9.14, which is a flexible and realistic open-source autonomous vehicle simulator. The simulator offers a wide range of sensors, environmental configurations, and varying rendering configurations. As noted earlier, we take several important considerations into account while curating SKYSCENES images. These include strategies for obtaining diverse synthetic data and embedding real-world irregularities, avoiding correlated images, addressing skewed class representations, and more. In this section, we first discuss such desiderata and then describe our procedural image curation algorithm. Finally, we describe different aspects of the curated dataset.

3.1 (Synthetic) Aerial Image Desiderata

Before investigating the image curation pipeline, we first outline a set of desiderata taken into account while curating synthetic aerial images in SKYSCENES.

1. **Viewpoint Reproducibility:** Critical to understanding how models respond to changing conditions is the ability to evaluate them under scenarios where only one variable is altered. However, any effort to do so in the real-world would be uncontrolled, due to its dynamic (constantly changing) nature.

³ <https://carla.org/>

In contrast, simulated data allows us to do so by providing control over image generation conditions. Unlike certain existing aerial datasets that do not support this feature (see Table. 1), we do so in SKYSCENES by additionally storing comprehensive metadata for each viewpoint (and image), including details about camera world coordinates, orientation, and all movable/immovable actors and objects in the scene. We couple this with rigorous consistency checks for image generation that verify the number of actors, their location, sensor height, pitch, etc. This meticulous approach enables us to reproduce the same viewpoint under multiple conditions effortlessly.

2 . Adequate Representation of Tail Classes: Unlike ground-view datasets, pixel distribution of classes in aerial images is substantially more long-tailed (see Fig. 2 (a); classes with smaller object size, **humans**). This substantial difference in class proportions severely affects the performance of tail classes in aerial datasets when compared to ground-view datasets (see Fig. 2 (b)), thus making visual recognition tasks harder. To counter this, we consider structured spawning of **humans** to ensure adequate representation (see Sec. 3.2).

3. Adequate Height Variations: Aerial images are captured at different altitudes to meet specific needs. Lower altitudes (5-15m) are optimal for high-resolution photography and detailed inspections. Altitudes ranging from 30m-50m strike a balance between fine-grained detail and a broader perspective, making them ideal for surveillance. Altitudes above 50m are suitable for capturing extensive areas, making them ideal for surveying and mapping. Existing datasets (synthetic or real) often focus on “specific” altitude ranges (see Table. 1, Image Capture columns), limiting their adaptability to different scenarios. With SKYSCENES, our aim is to provide flexibility in altitude sampling, thus accommodating various real-world requirements. We curate SKYSCENES images at heights of 15m, 35m, and 60m. Additionally, recognizing imperfections in real-world actuation, we induce slight jitter in the height values ($\Delta h \sim \mathcal{N}(1, 2.5m)$) to simulate realistic data sampling.

4. Adequate Pitch Variations: Similar to height, aerial images can be captured from 3 primary perspectives or pitch angles (θ): nadir ($\theta = 90^\circ$), oblique ($\theta \in (0^\circ, 90^\circ)$), or forward ($\theta = 0^\circ$) views (see Table. 1, Image Capture columns). The nadir view (directly perpendicular to the ground plane), preserves object scale while forward views are well-suited for tasks like UAV navigation and obstacle detection. Oblique views, on the other hand, capture objects from a side profile, aiding object recognition and providing valuable context and depth perspective often lost in nadir and forward views. To ensure widespread utility, SKYSCENES data generation process is designed to support all these viewing angles, with a particular emphasis on oblique views (the most common one). Similar to height, pitch variations allow models trained on SKYSCENES to generalize to different viewpoint variations. We use $\theta = 45^\circ$ and 60° for oblique-views and introduce jitter ($\Delta\theta \sim \mathcal{N}(1, 5^\circ)$) to mimic real-world data sampling.

5. Adequate Map Variations: In addition to sensor locations, it is equally important to curate aerial images across diverse scene layouts. To ensure adequate map variations, we gather images from 8 different CARLA [10] towns (can be categorized as *urban* or *rural*), which provide substantial variations in the observed

scene. These towns differ in layouts, size, road map design, building design, and vegetation cover. Fig. 4 illustrates how images curated from different towns in CARLA [10] differ in class distributions.

6. Adequate Weather & Daytime Variations: Training robust perception models using SKYSCENES that generalize to unforeseen environmental conditions necessitates the curation of annotated images encompassing various weather and daytime scenarios. To accomplish this, we generate SKYSCENES images from identical viewpoints under 5 different variations – ClearNoon, ClearSunset, MidRainNoon, ClearNight, and CloudyNoon.⁴ Generating images in different conditions from the same perspectives allows us to (1) leverage diverse data for improved generalization and (2) systematically investigate the susceptibility of trained models to variations in daytime and weather conditions.

7. Fine-grained Annotations: To support a host of different computer vision tasks (segmentation, detection, multimodal recognition), we curate all SKYSCENES images with dense semantic, instance segmentation and depth annotations. We provide semantic annotations for a wide vocabulary of 28 classes to support broad applicability (see Fig. 1 column 4 for an example).

3.2 SKYSCENES Image Generation

We generate SKYSCENES images from CARLA [10] by taking the previously mentioned considerations into account. Curating images from CARLA [10] broadly consists of two key steps: (1) positioning the agent camera in an aerial perspective and (2) procedurally guiding the agent within the scene to capture images. We accomplish the first by mimicking a UAV perspective in CARLA [10] by positioning the ego vehicle (with RGB, semantic and depth sensors) based on specified (high) altitude (h) and pitch (θ) values to generate aerial views (see Fig. 2a).⁵ Once positioned, the agent is translated by fixed amounts to traverse the scene and capture images from various viewpoints (detailed in Sec. B.1 in the appendix). Initially, we generate 70 data points for each of the 8 town variations under ClearNoon conditions using the baseline $h = 35\text{m}$, $\theta = 45^\circ$ setting. Subsequently, following the traversal algorithm (see Sec. B.1 in the appendix), we re-generate these datapoints across 5 weather conditions and 12 height/pitch variations, resulting in $70 \times 8 \times 5 \times 12 = 33,600$ images.

Checks and Balances. Additionally, we ensure the following checks and balances while curating SKYSCENES images.

▷ **Avoiding Overly Correlated Frames for Viewpoints.** CARLA [10] uses a traffic manager with a PID controller to control the egocentric vehicle based on current pose, speed, and a list of waypoints at every pre-defined time step. Curating images at every time step (or tick) results in highly correlated frames with

⁴ Note that CARLA [10] provides 14 such conditions but we use only 5 such conditions in this preliminary version of SKYSCENES.

⁵ This also requires setting other scenes – weather, daytime, etc. – and camera (notably the $\text{FoV} = 110^\circ$ (field of view) and image resolution = 2160x1440) parameters.

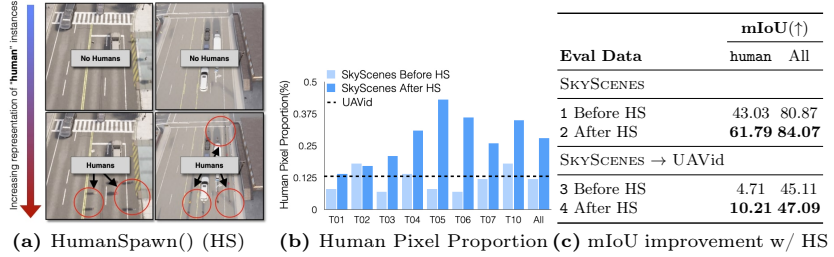


Fig. 3: SKYSCENES w/ HumanSpawn() increases representation of humans and improves SKYSCENES → UAVid (S→U) performance. (a) Incorporating HumanSpawn() in the image generation pipeline for SKYSCENES increases the proportion of **humans** in snapshots ([Top]→[Bottom]). (b) Increased representation of **humans** across all the layout variations in SKYSCENES after HumanSpawn(), with the dotted line representing the proportion of **humans** in UAVid (c) Training on HumanSpawn (HS) SKYSCENES images improves the model’s ability to recognize **humans** (improved mIoU). T = Town.

little change in object position. Since overly correlated frames are not very useful when training models for static scene understanding, we move the camera by a fixed distance multiple times before saving a frame. This also helps with moving dynamic actors by a considerable amount in the scene. Additionally, pedestrian objects are regenerated before saving an image, which adds randomness to the spawning and placement of pedestrians, reducing the correlation between frames.

▷ **Adequate Representation of humans.** Real-world scenes often exhibit a long-tailed distribution in pixel proportions, particularly in aerial images where variations in object sizes and camera positions contribute to significant under-representation of the tail classes (in Fig. 2, for the shared set of classes across UAVid [27] (aerial) and Cityscapes [8] (ground), we can see that the class distributions are different and aerial images are significantly more heavy-tailed). As a result, naively spawning **humans** (rarest class) in CARLA [10] is detrimental for eventual task performance – for the **human** class, a SKYSCENES trained DAFormer [16] (with HRDA [17] source training; MiT-B5 [55] backbone) model leads to an in-distribution performance of 43.03 mIoU and out-of-distribution (SKYSCENES → UAVid [27]) performance of 4.71 mIoU. To counter this under-representation issue, we design an algorithm, HumanSpawn() (see Sec. B.1 in appendix), to explicitly spawn more **human** instances while curating SKYSCENES images. HumanSpawn() increases **human** instances by 40 – 200 per snapshot, improving the proportion of densely annotated **humans** in SKYSCENES by approximately 10 times (see Fig. 3 (a) & Fig. 3 (b)). This improvement in **human** representation is also evident in eventual task performance, with in-distribution and out-of-distribution mIoUs for **humans** increasing from 43.03 to 61.79 (+18.76) and 4.71 to 10.21 (+5.50) respectively (see Table. 3 (c)).

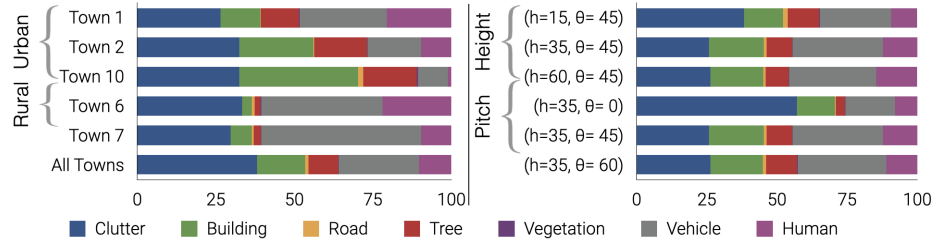


Fig. 4: Class-distribution Diversity in SKYSCENES. We show how the distribution of densely-annotated pixels varies across different SKYSCENES conditions. **[Left]** Class distribution varies substantially within and across urban and rural map layouts. **[Right]** Similarly, for the same SKYSCENES layouts (and viewpoints) class distribution varies substantially across different height and pitch values.

3.3 SKYSCENES: Dataset Details

Annotations. We provide semantic, instance and depth annotations for every image in SKYSCENES. Semantic annotations in SKYSCENES by default are across 28 classes. These are building, fence, pedestrian, pole, roadline (markings on road), road, sidewalk, vegetation, cars, wall, traffic sign, sky, bridge, railtrack, guardrail, traffic light, water, terrain, rider, bicycle, motorcycle, bus, truck and others (see Fig. 1 for an example and Sec. B.2 in appendix for definitions)

Training, Validation and Test Splits. SKYSCENES has 70 images per town (across 8 towns) for each of the 5 weather and daytime conditions, and 12 height & pitch combinations, resulting in a total of 33,600 images. We use 80% (26,880 images) of the dataset for training models, with 10% (3,360 images) each for validation and testing (see Sec. C.2 in appendix).

Class Distribution(s). In Fig. 4, we highlight how the distribution of classes changes across variations within SKYSCENES—rural and urban map layouts and height and pitch specifications. SKYSCENES exhibits substantial diversity in class distributions across such conditions, allowing these individual conditions to serve as diagnostic splits to assess model sensitivity (see Sec. 4.2).

4 Experiments

We conduct semantic segmentation experiments with SKYSCENES to assess a few different factors. First, we check if training on SKYSCENES is beneficial for real-world transfer. Second, we check if SKYSCENES can augment real-world training data in low and full shot regimes. Third, we check if variations in SKYSCENES can be used to assess the sensitivity of trained models to changing conditions. Finally, we check if using additional modality information (depth) can help improve aerial scene understanding.

Synthetic and Real Datasets. We compare real-world generalization performance of training on SKYSCENES with SYNDRONE [42], a recently proposed synthetic aerial dataset also curated from CARLA [10] featuring 3 different (h, θ)

Source	(Target) Real-World mIoU (\uparrow)			
	UAVid	AEROGRAPHES	ICG	DRONE
DeepLabv2 (R-101) [4]				
1 SYNDRONE	39.86	24.50	8.20	
2 SKYSCENES	41.82	26.94	15.14	
DAFormer (MiT-B5) [17]				
3 SYNDRONE	42.31	30.53	15.92	
4 SKYSCENES	47.09	40.72	25.91	
Rein (DINOv2)				
5 SYNDRONE	54.92	40.28	20.01	
6 SKYSCENES	54.19	43.96	28.10	

Table 2: Models trained on SKYSCENES generalize well to the real-world. We train semantic segmentation models (DeepLabv2 [4], DAFormer [16], Rein [54]) on SKYSCENES, SYNDRONE [42], and real datasets and show how training models on SKYSCENES provides better out-of-the-box generalization to multiple real-world datasets.

Source	(Target) Real-World IoU (\uparrow)			
	UAVid	AEROGRAPHES	ICG	DRONE
DAFormer (MiT-B5) [17]				
1 SYNDRONE	42.52	8.27	49.77	0.77
2 SKYSCENES	63.64	10.21	80.99	3.09
Rein (DINOv2) [54]				
3 SYNDRONE	68.68	21.6	84.2	10.29
4 SKYSCENES	75.14	25.52	87.71	21.67
	50.91	77.93		

Table 3: SKYSCENES training exhibits strong real-world generalization for tail classes. We show how DAFormer [16] and Rein [54] models trained on SKYSCENES exhibit improved real-world generalization compared to those trained on SYNDRONE [42] for under-represented tail classes (vehicles and humans). SKYSCENES training facilitates better recognition of tail class instances.

conditions across 8 different map layouts. We assess performance on 3 real-world aerial datasets – UAVid [27], AEROGRAPHES [34], ICG DRONE [20]. Since different datasets have different class vocabularies and definitions, for our experiments, we adapt the class vocabulary of the synthetic source dataset to that of the target real-world datasets (see Sec. C.1 in appendix for class merging and assignment schemes). Additionally, since different real aerial datasets have been captured from different heights and pitch angles, we train models on (h, θ) subsets of synthetic datasets that are aligned with corresponding real data (h, θ) conditions. We provide additional details for the real aligned synthetic data selection and model evaluation in Sec. D.3 in the appendix.

Models. We use (1) CNN – DeepLabv2 [4] (ResNet-101 [14]), (2) transformer – DAFormer [16] (with HRDA [17] source training; MiT-B5 [55] backbone) and (3) Vision Foundation Model – Rein [54] (LoRA [19] fine-tuned Dino-V2 [36] backbone) based semantic segmentation architectures for our experiments. We provide implementation details for our experiments in Sec. C in appendix.

4.1 SKYSCENES → Real Transfer

▷ **SKYSCENES trained models generalize well to real-settings.** In Table. 2, we show how models trained on SKYSCENES exhibit strong out-of-the box generalization performance on multiple real world datasets. We find that SKYSCENES pretraining exhibits stronger generalization compared to SYNDRONE [42] across both CNN and transformer segmentation backbones. In Table. 3, we show how generalization improvements are more pronounced for under-represented tail classes (vehicles and humans). Comparison across all classes is provided in Tables 11, 12 and 13 in appendix.

Source	(Target) Real World mIoU (↑)				
	5%	10%	25%	50%	100%
DeepLabv2 (R-101) [4]					
1 Only Real	48.25	55.29	62.86	66.81	68.53
2 SKYSCENES + Real (JT)	59.27	64.15	68.11	70.18	69.51
3 SKYSCENES + Real (FT)	53.67	60.61	65.57	68.54	69.70
DAFormer (MiT-B5) [17]					
4 Only Real	60.59	65.63	70.31	72.16	72.47
5 SKYSCENES + Real (JT)	62.97	67.58	70.20	71.83	72.25
6 SKYSCENES + Real (FT)	60.90	66.79	70.41	72.63	73.02
Rein (DINOv2) [54]					
7 Only Real	64.04	71.87	73.87	76.05	76.55
8 SKYSCENES + Real (JT)	69.15	73.54	75.07	76.08	76.54
9 SKYSCENES + Real (FT)	70.07	73.99	75.01	76.44	76.89

Table 4: SKYSCENES augmented real data improves performance in low shot regimes. We compare DeepLabv2 [4], DAFormer [16], and Rein [54] models trained using varying percentages of labeled UAVid [27] images. Models are either trained jointly multimodal segmentation architectures on SKYSCENES and UAVid (JT) or pre- with MiT-B5 [55] backbones using RGB trained on SKYSCENES and finetuned on and RGB+D data in SKYSCENES. Ad- UAVid (FT). Augmenting real data with ditional sensors improve aerial scene un- SKYSCENES enhances real-world general- derstanding significantly across various ization in low-shot scenarios.



Fig. 5: SKYSCENES RGB Images and corresponding depth images generated using depth sensor for $h = 35$, $\theta = 45^\circ$, and ClearNoon setting across four different town layouts.

Sensors	SKYSCENES Test IoU (↑)						Avg
	clutter	building	road	tree	low-veg.	vehicle	
1 RGB	87.80	94.54	94.07	88.03	69.37	82.89	43.35
2 RGB+D	90.64	95.97	94.87	89.41	74.36	86.87	50.47
							83.22

Table 5: Multi-modal Segmentation in SKYSCENES. We evaluate M3L [28] with MiT-B5 [55] backbones using RGB trained on and RGB+D data in SKYSCENES. Ad- SKYSCENES enhances real-world general- derstanding significantly across various classes in UAVid [27].

▷ **SKYSCENES can augment real training data.** In addition to zero-shot real-world generalization, akin to other synthetic aerial datasets, we also show how SKYSCENES is useful as additional training data when labeled real-world data is available. In Table. 4, for SKYSCENES → UAVid [27], we compare models trained only using 5%, 10%, 25%, 50%, 100% of the 200 UAVid [27] training images with counterparts that were either pretrained using SKYSCENES data or additionally supplemented with SKYSCENES data at training time. We find that in low-shot regimes (when little “real” world data is available), SKYSCENES data (either explicitly via joint training or implicitly via finetuning) is beneficial in improving recognition performance (see Sec. D.5 of appendix).

4.2 SKYSCENES as a Diagnostic Framework

As noted earlier, the images we curate in SKYSCENES contain several variations – ranging from 5 different weather and daytime conditions, rural and urban map layouts, and 12 different height and pitch combinations (see Fig. 4 for variations in class distributions). We curate images under such diverse conditions in a *controlled manner* – ensuring the same spatial coordinates for (h, θ) variations, same spatial coordinates and (h, θ) settings across different weather and daytime conditions, the same number of images across layouts.

This allows us to assess the sensitivity of trained models to one factor of variation (h, θ , daytime, weather, map layout) by changing that specific aspect. We summarize some takeaways from such experiments in Table. 6.

Test mIoU (\uparrow)			Test mIoU (\uparrow)			Test mIoU (\uparrow)			Test mIoU (\uparrow)						
Train	Clear	Cloudy	Train	Noon	Sunset	Train	Rural	Urban	Height	$\theta = 0^\circ$	$\theta = 45^\circ$	$\theta = 60^\circ$	$\theta = 90^\circ$		
1 Clear	73.91	73.59	69.95	1 Noon	73.91	71.16	35.60	1 Rural	58.00	35.90	1 $h = 15\text{m}$	48.50	50.71	45.22	42.21
2 Cloudy	69.60	74.02	69.14	2 Sunset	63.16	66.53	39.36	2 Urban	38.99	73.16	2 $h = 35\text{m}$	50.49	55.74	57.11	52.19
3 Rainy	69.00	73.36	72.62	3 Night	52.00	57.35	70.36	3 Map			3 $h = 60\text{m}$	45.33	49.79	50.37	44.62
(a) Weather Variation			(b) Daytime Variation			(c) Map Variation			(d) Height & Pitch Variation						

Table 6: Model Sensitivity to Changing Conditions. We show how changing conditions (weather, daytime, map, viewpoint) in SKYSCENES can serve as diagnostic test splits to assess the sensitivity of trained DAFormer [16] semantic segmentation models. In (a) and (b), we evaluate models trained under different weather and daytime conditions across the same conditions. In (c), we evaluate models trained on rural and urban scenes across the same layouts. In (d), we evaluate a model trained on moderate height, pitch settings ($h = 35\text{m}, \theta = 45^\circ$) across different (h, θ) variations. Best numbers across each row condition is highlighted in blue.

In Table. 6 (a), we show how models trained in a certain weather condition are best at generalizing to the same condition at test-time. We make similar observations for daytime variations in Table. 6 (b). In Table. 6 (c), we show how models trained in rural conditions fail to perform well in urban test-time conditions and vice-versa. In Table. 6 (d), we evaluate a model trained under moderate ($h = 35\text{m}, \theta = 45^\circ$) conditions under different (h, θ) variations. We find that as altitudes increase, trained models are better at recognizing objects from oblique ($\theta \in (0^\circ, 90^\circ)$) viewpoints. We provide exhaustive quantitative comparisons in Sec. D.6 in the appendix.

4.3 SKYSCENES Enables Multi-modal Dense Prediction

Sensors on UAVs in deployable settings often include modalities beyond RGB cameras, such as depth sensors. These additional modalities can significantly enhance aerial scene understanding. In Table. 5, we investigate the impact of augmenting RGB data with depth observations from SKYSCENES viewpoints on aerial semantic segmentation using M3L [28], a multimodal segmentation model. Similar to our DAFormer [16] experiments, we consider a SegFormer equivalent version of M3L [28] (with an MiT-B5 [55] backbone). We test RGB and RGB+D models trained under ($h = 35, \theta = 45^\circ$) (moderate viewpoint) conditions on SKYSCENES and find that incorporating additional Depth observations can substantially improve recognition performance. This demonstrates that images in SKYSCENES can be used to train multimodal scene-recognition models.

5 Conclusion

We introduce SKYSCENES, a large-scale densely-annotated dataset of synthetic aerial scene images curated from unmanned aerial vehicle (UAV) perspectives. SKYSCENES images are generated using CARLA by situating an agent aerially and procedurally tele-operating it through the scene to capture frames with

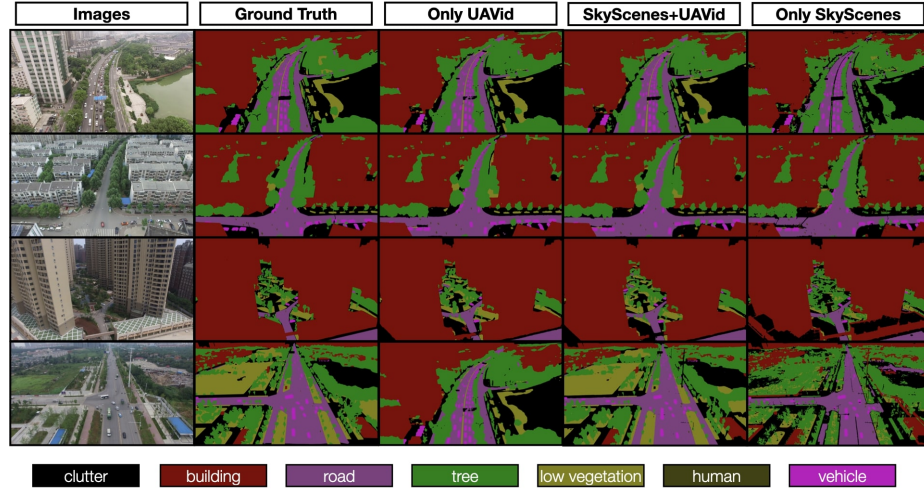


Fig. 6: UAVid, SKYSCENES + UAVid and SKYSCENES → UAVid semantic segmentation predictions Predictions on randomly selected UAVid [27] validation images by a Rein [54] model trained on UAVid and SKYSCENES. Columns 1 and 2 show the original image and its ground truth. Columns 3, 4, and 5 display predictions from models trained exclusively on UAVid, jointly on SKYSCENES and UAVid, and exclusively on SKYSCENES, respectively.

semantic, instance, and depth annotations. Our careful curation process ensures that SKYSCENES images span across diverse weather, daytime, map, height, and pitch conditions, with accompanying metadata that enables reproducing the same viewpoint (spatial coordinates and perspective) under differing conditions.

Through our experiments, we demonstrate that: (1) SKYSCENES-trained models generalize well to real-world settings, (2) SKYSCENES augments labeled real-world data in low-shot scenarios, (3) SKYSCENES serves as a diagnostic tool for assessing model sensitivity to varied conditions, and (4) incorporating additional sensors like depth enhances multi-modal aerial scene understanding.

We aim to enhance SKYSCENES with improved realism, additional anticipated edge cases, and support for 3D perception tasks aligning with advancements in our simulator (additional details in Sec. F of appendix) We have publicly released the dataset and associated generation code and hope that our experimental findings encourage further research using SKYSCENES for aerial scenes.

Acknowledgements. We would like to thank Sean Foley for his contributions to the early efforts and discussions of this project. This work has been partially sponsored by NASA University Leadership Initiative (ULI) #80NSSC20M0161, ARL, and NSF #2144194.

References

1. Cai, W., Jin, K., Hou, J., Guo, C., Wu, L., Yang, W.: Vdd: Varied drone dataset for semantic segmentation (2023)
2. Chattopadhyay, P., Hoffman, J., Mottaghi, R., Kembhavi, A.: Robustnav: Towards benchmarking robustness in embodied navigation. International Conference in Computer Vision (ICCV) (2021)
3. Chauhan, A., Wasim, M., Mohanty, S., Pandey, P.C., Pandey, M., Maurya, N.K., Rankavat, S., Dubey, S.B.: Chapter 10 - earth observation applications for urban mapping and monitoring: research prospects, opportunities and challenges. In: Kumar, A., Srivastava, P.K., Saikia, P., Mall, R.K. (eds.) Earth Observation in Urban Monitoring, pp. 197–229. Earth Observation, Elsevier (2024). <https://doi.org/https://doi.org/10.1016/B978-0-323-99164-3.00007-0>, <https://www.sciencedirect.com/science/article/pii/B9780323991643000070>
4. Chen, L.C., Papandreou, G., Kokkinos, I., Murphy, K., Yuille, A.L.: Deeplab: Semantic image segmentation with deep convolutional nets, atrous convolution, and fully connected crfs (2017)
5. Chen, L., Liu, F., Zhao, Y., Wang, W., Yuan, X., Zhu, J.: Valid: A comprehensive virtual aerial image dataset. In: 2020 IEEE International Conference on Robotics and Automation (ICRA). pp. 2009–2016 (2020). <https://doi.org/10.1109/ICRA40945.2020.9197186>
6. Chen, Y., Wang, Y., Lu, P., Chen, Y., Wang, G.: Large-scale structure from motion with semantic constraints of aerial images. In: Chinese Conference on Pattern Recognition and Computer Vision (PRCV). pp. 347–359. Springer (2018)
7. Chiang, C.Y., Barnes, C., Angelov, P., Jiang, R.: Deep learning-based automated forest health diagnosis from aerial images. IEEE Access **8**, 144064–144076 (2020). <https://doi.org/10.1109/ACCESS.2020.3012417>
8. Cordts, M., Omran, M., Ramos, S., Rehfeld, T., Enzweiler, M., Benenson, R., Franke, U., Roth, S., Schiele, B.: The cityscapes dataset for semantic urban scene understanding. In: Proceedings of the IEEE conference on computer vision and pattern recognition. pp. 3213–3223 (2016)
9. Demir, I., Koperski, K., Lindenbaum, D., Pang, G., Huang, B., Basu, S., Hughes, F., Tuia, D., Raska, R., Kressner, A., et al.: Deepglobe 2018: A challenge to parse the earth through satellite images. In: IEEE Conference on Computer Vision and Pattern Recognition Workshops. pp. 172–172 (2018)
10. Dosovitskiy, A., Ros, G., Codevilla, F., Lopez, A., Koltun, V.: Carla: An open urban driving simulator. In: Conference on robot learning. pp. 1–16. PMLR (2017)
11. Du, D., Qi, Y., Yu, H., Yang, Y., Duan, K., Li, G., Zhang, W., Huang, Q., Tian, Q.: The unmanned aerial vehicle benchmark: Object detection and tracking. In: Proceedings of the European conference on computer vision (ECCV). pp. 370–386 (2018)
12. Fonder, M., Droogenbroeck, M.V.: Mid-air: A multi-modal dataset for extremely low altitude drone flights. In: Conference on Computer Vision and Pattern Recognition Workshop (CVPRW) (June 2019)
13. Frueh, C., Sammon, R., Zakhori, A.: Automated texture mapping of 3d city models with oblique aerial imagery. In: Proceedings. 2nd International Symposium on 3D Data Processing, Visualization and Transmission, 2004. 3DPVT 2004. pp. 396–403 (2004). <https://doi.org/10.1109/TDPVT.2004.1335266>
14. He, K., Zhang, X., Ren, S., Sun, J.: Deep residual learning for image recognition. In: Proceedings of the IEEE conference on computer vision and pattern recognition. pp. 770–778 (2016)

15. Heusel, M., Ramsauer, H., Unterthiner, T., Nessler, B., Hochreiter, S.: Gans trained by a two time-scale update rule converge to a local nash equilibrium (2018), <https://arxiv.org/abs/1706.08500>
16. Hoyer, L., Dai, D., Gool, L.V.: Daformer: Improving network architectures and training strategies for domain-adaptive semantic segmentation (2022)
17. Hoyer, L., Dai, D., Gool, L.V.: Hrda: Context-aware high-resolution domain-adaptive semantic segmentation (2022)
18. Hoyer, L., Dai, D., Wang, H., Gool, L.V.: Mic: Masked image consistency for context-enhanced domain adaptation (2023)
19. Hu, E.J., Shen, Y., Wallis, P., Allen-Zhu, Z., Li, Y., Wang, S., Wang, L., Chen, W.: Lora: Low-rank adaptation of large language models (2021)
20. Institute of Computer Graphics and Vision, Graz University of Technology: Semantic drone dataset. <http://dronedataset.icg.tugraz.at>
21. Kedys, J., Tchappi, I., Najjar, A.: Uavs for disaster management - an exploratory review. *Procedia Computer Science* **231**, 129–136 (2024). <https://doi.org/https://doi.org/10.1016/j.procs.2023.12.184>, <https://www.sciencedirect.com/science/article/pii/S1877050923021968>, 14th International Conference on Emerging Ubiquitous Systems and Pervasive Networks / 13th International Conference on Current and Future Trends of Information and Communication Technologies in Healthcare (EUSPN/ICTH 2023)
22. Kingma, D.P., Ba, J.: Adam: A method for stochastic optimization. arXiv preprint arXiv:1412.6980 (2014)
23. Lin, L., Liu, Y., Hu, Y., Yan, X., Xie, K., Huang, H.: Capturing, reconstructing, and simulating: the urbanscene3d dataset. In: ECCV. pp. 93–109 (2022)
24. Liu, T., Yang, X.: Monitoring land changes in an urban area using satellite imagery, gis and landscape metrics. *Applied Geography* **56**, 42–54 (2015). <https://doi.org/https://doi.org/10.1016/j.apgeog.2014.10.002>, <https://www.sciencedirect.com/science/article/pii/S0143622814002306>
25. Lopez-Campos, R., Martinez-Carranza, J.: Espada: Extended synthetic and photogrammetric aerial-image dataset. *IEEE Robotics and Automation Letters* **6**(4), 7981–7988 (2021). <https://doi.org/10.1109/LRA.2021.3101879>
26. Loschilov, I., Hutter, F.: Decoupled weight decay regularization (2019)
27. Lyu, Y., Vosselman, G., Xia, G.S., Yilmaz, A., Yang, M.Y.: Uavid: A semantic segmentation dataset for uav imagery. *ISPRS journal of photogrammetry and remote sensing* **165**, 108–119 (2020)
28. Maheshwari, H., Liu, Y.C., Kira, Z.: Missing modality robustness in semi-supervised multi-modal semantic segmentation (2023)
29. Morgan, G.R., Wang, C., Li, Z., Schill, S.R., Morgan, D.R.: Deep learning of high-resolution aerial imagery for coastal marsh change detection: A comparative study. *ISPRS International Journal of Geo-Information* **11**(2) (2022). <https://doi.org/10.3390/ijgi11020100>, <https://www.mdpi.com/2220-9964/11/2/100>
30. Mueller, M., Smith, N., Ghanem, B.: A benchmark and simulator for uav tracking. In: Leibe, B., Matas, J., Sebe, N., Welling, M. (eds.) *Computer Vision – ECCV 2016*. pp. 445–461. Springer International Publishing, Cham (2016)
31. Munawar, H.S., Ullah, F., Qayyum, S., Khan, S.I., Mojtabaei, M.: Uavs in disaster management: Application of integrated aerial imagery and convolutional neural network for flood detection. *Sustainability* **13**(14) (2021). <https://doi.org/10.3390/su13147547>, <https://www.mdpi.com/2071-1050/13/14/7547>
32. Neuhold, G., Ollmann, T., Bulò, S.R., Kontschieder, P.: The mapillary vistas dataset for semantic understanding of street scenes. In: *2017 IEEE Interna-*

tional Conference on Computer Vision (ICCV). pp. 5000–5009 (2017). <https://doi.org/10.1109/ICCV.2017.534>

33. Nguyen, K., Fookes, C., Sridharan, S., Tian, Y., Liu, F., Liu, X., Ross, A.: The state of aerial surveillance: A survey (2022)
34. Nigam, I., Huang, C., Ramanan, D.: Ensemble knowledge transfer for semantic segmentation. In: Proceedings of the 2018 IEEE Winter Conference on Applications of Computer Vision. pp. 916–924. IEEE (2018)
35. Oh, S., Hoogs, A., Perera, A., Cuntoor, N., Chen, C.C., Lee, J.T., Mukherjee, S., Aggarwal, J.K., Lee, H., Davis, L., Squires, E., Wang, X., Ji, Q., Reddy, K., Shah, M., Vondrick, C., Pirsiavash, H., Ramanan, D., Yuen, J., Torralba, A., Song, B., Fong, A., Roy-Chowdhury, A., Desai, M.: A large-scale benchmark dataset for event recognition in surveillance video. In: CVPR 2011. pp. 3153–3160 (2011). <https://doi.org/10.1109/CVPR.2011.5995586>
36. Oquab, M., Darabet, T., Moutakanni, T., Vo, H., Szafraniec, M., Khalidov, V., Fernandez, P., Haziza, D., Massa, F., El-Nouby, A., Assran, M., Ballas, N., Galuba, W., Howes, R., Huang, P.Y., Li, S.W., Misra, I., Rabbat, M., Sharma, V., Synnaeve, G., Xu, H., Jegou, H., Mairal, J., Labatut, P., Joulin, A., Bojanowski, P.: Dinov2: Learning robust visual features without supervision (2024)
37. Otal, H.T., Zavar, E., Binder, S.B., Greer, A., Canbaz, M.A.: Harnessing deep learning and satellite imagery for post-buyout land cover mapping (2024)
38. Peng, X., Usman, B., Kaushik, K., Hoffman, J., Wang, D., Saenko, K., Zhang, Y.: Visda: The visual domain adaptation challenge. In: IEEE International Conference on Computer Vision. pp. 1685–1692 (2017)
39. Prokaj, J., Medioni, G.: Persistent tracking for wide area aerial surveillance. In: Proceedings of the IEEE Conference on Computer Vision and Pattern Recognition (CVPR) (June 2014)
40. Rahmehoonfar, M., Chowdhury, T., Sarkar, A., Varshney, D., Yari, M., Murphy, R.: Floodnet: A high resolution aerial imagery dataset for post flood scene understanding (2020)
41. Ren, T., Liu, S., Zeng, A., Lin, J., Li, K., Cao, H., Chen, J., Huang, X., Chen, Y., Yan, F., Zeng, Z., Zhang, H., Li, F., Yang, J., Li, H., Jiang, Q., Zhang, L.: Grounded sam: Assembling open-world models for diverse visual tasks (2024)
42. Rizzoli, G., Barbato, F., Caligiuri, M., Zanuttigh, P.: Syndrone—multi-modal uav dataset for urban scenarios. arXiv preprint arXiv:2308.10491 (2023)
43. Ros, G., Sellart, L., Materzynska, J., Vazquez, D., Lopez, A.M.: The synthia dataset: A large collection of synthetic images for semantic segmentation of urban scenes. In: Proceedings of the IEEE conference on computer vision and pattern recognition. pp. 3234–3243 (2016)
44. Rottensteiner, F., Sohn, G., Jung, J., Gerke, M., Baillard, C., Bénitez, S., Breitkopf, U.: The isprs benchmark on urban object classification and 3d building reconstruction. ISPRS Annals of Photogrammetry, Remote Sensing and Spatial Information Sciences **I-3** (07 2012). <https://doi.org/10.5194/isprsaannals-I-3-293-2012>
45. Sakaridis, C., Dai, D., Van Gool, L.: Guided curriculum model adaptation and uncertainty-aware evaluation for semantic nighttime image segmentation. In: The IEEE International Conference on Computer Vision (ICCV) (2019)
46. Sankaranarayanan, S., Balaji, Y., Castillo, C.D., Chellappa, R.: Generate to adapt: Aligning domains using generative adversarial networks. In: The IEEE Conference on Computer Vision and Pattern Recognition (CVPR) (June 2018)
47. Scanlon, M.: Semantic Annotation of Aerial Images using Deep Learning, Transfer Learning, and Synthetic Training Data. Ph.D. thesis, University of Galway (09 2018)

48. Shah, S., Dey, D., Lovett, C., Kapoor, A.: Airsim: High-fidelity visual and physical simulation for autonomous vehicles. In: Field and Service Robotics (2017), <https://arxiv.org/abs/1705.05065>
49. Sun, T., Segu, M., Postels, J., Wang, Y., Gool, L.V., Schiele, B., Tombari, F., Yu, F.: Shift: A synthetic driving dataset for continuous multi-task domain adaptation (2022)
50. Testolina, P., Barbato, F., Michieli, U., Giordani, M., Zanuttigh, P., Zorzi, M.: Selma: Semantic large-scale multimodal acquisitions in variable weather, daytime and viewpoints (2022)
51. Tong, X.Y., Xia, G.S., Lu, Q., Shen, H., Li, S., You, S., Zhang, L.: Land-cover classification with high-resolution remote sensing images using transferable deep models. *Remote Sensing of Environment* **237**, 111322 (2020)
52. VidalMata, R.G., Banerjee, S., RichardWebster, B., Albright, M., Davalos, P., McCloskey, S., Miller, B., Tambo, A., Ghosh, S., Nagesh, S., Yuan, Y., Hu, Y., Wu, J., Yang, W., Zhang, X., Liu, J., Wang, Z., Chen, H.T., Huang, T.W., Chin, W.C., Li, Y.C., Lababidi, M., Otto, C., Scheirer, W.J.: Bridging the gap between computational photography and visual recognition. *IEEE Transactions on Pattern Analysis and Machine Intelligence* **43**(12), 4272–4290 (2021). <https://doi.org/10.1109/TPAMI.2020.2996538>
53. Wang, W., Zhu, D., Wang, X., Hu, Y., Qiu, Y., Wang, C., Hu, Y., Kapoor, A., Scherer, S.: Tartanair: A dataset to push the limits of visual slam (2020), <https://arxiv.org/abs/2003.14338>
54. Wei, Z., Chen, L., Jin, Y., Ma, X., Liu, T., Ling, P., Wang, B., Chen, H., Zheng, J.: Stronger, fewer, & superior: Harnessing vision foundation models for domain generalized semantic segmentation (2024)
55. Xie, E., Wang, W., Yu, Z., Anandkumar, A., Alvarez, J.M., Luo, P.: Segformer: Simple and efficient design for semantic segmentation with transformers. *Advances in Neural Information Processing Systems* **34**, 12077–12090 (2021)
56. Yu, F., Chen, H., Wang, X., Xian, W., Chen, Y., Liu, F., Madhavan, V., Darrell, T.: Bdd100k: A diverse driving dataset for heterogeneous multitask learning. In: Proceedings of the IEEE/CVF conference on computer vision and pattern recognition. pp. 2636–2645 (2020)
57. Zhu, P., Wen, L., Du, D., Bian, X., Fan, H., Hu, Q., Ling, H.: Detection and tracking meet drones challenge. *IEEE Transactions on Pattern Analysis and Machine Intelligence* pp. 1–1 (2021). <https://doi.org/10.1109/TPAMI.2021.3119563>

A Overview

The appendix is organized as follows. In Sec. B.1, we provide more details on different aspects of dataset – including the procedural image curation algorithm, algorithm to ensure appropriate representation of `human` instances, brief descriptions of all the classes in SKYSCENES and comparisons between data distribution of SKYSCENES and real datasets. Then, we describe experimental details in Sec. C – class-merging schemes used for our SKYSCENES → Real transfer experiments, train / val / test splits and experimental details for SKYSCENES diagnostic setup to probe model vulnerabilities. Sec. D provides more quantitative and qualitative experimental results.

B SKYSCENES Details

B.1 Image Generation Algorithms

We curate SKYSCENES using CARLA [10] 0.9.14 simulator. The generation process broadly consists of two key steps: (1) positioning the agent camera in an aerial perspective and (2) procedurally guiding the agent within the scene to capture images. We accomplish the first by mimicking a UAV perspective in CARLA [10] by positioning the ego vehicle (with RGB, semantic, depth and instance segmentation sensors) based on specified altitude (h) and pitch (θ) values to generate aerial views. This also requires setting other scene information like – town, weather, and daytime. The camera $\text{FoV} = 110^\circ$ (field of view) and $H \times W = 2160 \times 1440$ (image resolution) are also set.

To maintain the adequate representation of tail classes, especially for `humans` we incorporate structured spawning of `humans` using Algo. 2. CARLA [10] has a limit on the number of actors that can be spawned in a scene, which depends on factors such as the type and size of the town, number of lanes to spawn vehicles, and amount of sidewalk area. To overcome this limitation, we decided to bring the actors into the field of view of the camera instead of having them spread out in the scene. We developed an algorithm to find all the points to spawn pedestrians in the field of view using the camera location and spawn them like vehicles on roads. After taking a snapshot, we destroy the spawned pedestrians and repeat the process. Manual spawning not only increases the number of `human` instances and their proportion but also aligns their placement with real-world settings.

As SKYSCENES images are curated by teleoperating over entire maps (rural or urban) across multiple layouts that differ substantially in class distributions (Fig. 4 left in the paper). Since these frames are stored with corresponding geographical (layout identifier) and positional (spatial location) metadata, filtering data splits to avoid overlap across physical layout regions is always possible.

The steps involved in manual spawning instances of `humans` are summarized below:

- 1 Specify maximum number of `humans` to be spawned N_{\max}

Algorithm 1 SKYSCENES ImgGen ($z, \theta, \text{FoV}, H, W$)

```

1: # Initialize key CARLA parameters
2: Input:  $z$  (height),  $\theta$  (pitch),  $\text{FoV}$ ,  $H$ ,  $W$ 
3: # Initialize auxiliary CARLA parameters
4: Initialize:  $\text{MB} \leftarrow \text{Off}$  ▷ Turn off motion blur
5: Initialize: Post-process RGB  $\leftarrow \text{True}$  ▷ Turn on RGB post processing
6: Dataset:  $D = \{\cdot\}$ 
7: # Town and variation vocabulary
8:  $\mathbb{T} = \{T_i\}_{i=1}^M$  (Town),  $\mathbb{V} = \{V_i\}_{i=1}^N$  (Vars)
9: for  $T_i \in \mathbb{T}$  do
10:   for  $V_j \in \mathbb{V}$  do
11:     # Initialize CARLA scene
12:      $E \leftarrow \text{CARLA\_init}(T_i, V_j)$ 
13:     # Position Camera
14:      $\text{Init\_Sensor}(E, z, \theta, \text{FoV}, H, W, \text{MB})$ 
15:     # Spawn pedestrians, vehicles, etc.
16:      $\text{Spawn\_Actors}(E)$ 
17:     # Initialize Movement Steps
18:      $\Delta_{\text{step}} \leftarrow \Delta, N_{\text{steps}} \leftarrow N$ 
19:     for  $k \in N_{\text{steps}}$  do
20:       # Sample Frame
21:        $I \leftarrow \text{Sample\_Frame}(E)$ 
22:       # Get pixel-level annotations
23:        $I_{\text{anno}} \leftarrow \text{Get\_Anno}(E, I)$ 
24:       # Get metadata
25:        $I_{\text{meta}} \leftarrow \text{Get\_Meta}(E, I)$ 
26:       # Append to dataset
27:        $D \leftarrow D \cup \{(I, I_{\text{anno}}, I_{\text{meta}})\}$ 
28:       # Move camera by a fixed distance
29:        $\text{Move\_Camera}(E, \Delta_{\text{step}})$ 
30: Return:  $D$  (SKYSCENES data) ▷ Gathered Images

```

- 2 Get camera position (x, y, z) , set a pre-defined distance d to check for spawnable locations and execute the subroutine in Algo. 2. This will place the actors in the field of view till a junction or the next driving lane.
- 3 If at a junction, obtain the left and the right waypoints for every retrieved location at a distance of d to get the list of waypoints.
- 4 Using the waypoint from the end of the current lane, generate waypoints for the new main, left and right lanes by repeating the previous steps.
- 5 Repeat the above steps till $N_{\text{humans}} \leq N_{\text{max}}$

Once positioned, the agent is translated by fixed amounts to traverse the scene and capture images from various viewpoints. Initially, we generate 70 datapoints for each of the 8 town variations under ClearNoon conditions using the baseline $h = 35, \theta = 45^\circ$ setting. Subsequently, following the traversal algorithm (Algo. 1), we re-generate these datapoints across 5 weather conditions and 12 height/pitch variations, resulting in $70 \times 8 \times 5 \times 12 = 33,600$ images.

Algorithm 2 HumanSpawn (x, y, d, p_{gen})

```

1: # Initialize parameters
2: Input:  $x, y$  (camera position),  $d$  (distance between spawned instances),  $p_{\text{gen}}$  (spawn probability)
3: # Spawn locations
4:  $D_{\text{spawn}} = \{\cdot\}$ 
5: # Get candidate positions in front of the camera
6:  $\{(x, y)\}_{\text{front}} \leftarrow \text{get\_loc}(x, y, d)$  ▷ Current Lane
7: # Get candidate positions left of camera
8:  $\{(x, y)\}_{\text{left}} \leftarrow \text{get\_loc}(x - \Delta_{\text{left}}, y, d)$  ▷ Left Lane
9: # Get candidate positions right of camera
10:  $\{(x, y)\}_{\text{right}} \leftarrow \text{get\_loc}(x + \Delta_{\text{right}}, y, d)$  ▷ Right Lane
11:  $D_{\text{spawn}} \leftarrow \{(x, y)\}_{\text{front}} \cup \{(x, y)\}_{\text{left}} \cup \{(x, y)\}_{\text{right}}$ 
12: for  $(x, y) \in D_{\text{spawn}}$  do
13:   if random()  $\leq p_{\text{gen}}$  then
14:     # Spawn human
15:     spawn_human()

```

B.2 Class Descriptions

We provide semantic, instance, and depth annotations for every image in SKYSCENES. SKYSCENES provides dense semantic annotations for 28 classes. These are:

- **unlabeled**: elements/objects in the scene that have not been categorized in CARLA
- **other**: uncategorized elements
- **building**: includes houses, skyscrapers, and the elements attached to them.
- **fence**: wood or wire assemblies that enclose an area of ground
- **pedestrian**: humans that walk
- **pole**: vertically oriented pole and its horizontal components if any
- **roadline**: markings on road.
- **road**: lanes, streets, paved areas on which cars drive
- **sidewalk**: parts of ground designated for pedestrians or cyclists
- **vegetation**: trees, hedges, all kinds of vertical vegetation (ground-level vegetation is not included here).
- **cars**: cars
- **wall**: individual standing walls, not part of buildings
- **traffic sign**: signs installed by the state/city authority, usually for traffic regulation
- **sky**: open sky, including clouds and sun
- **ground**: any horizontal ground-level structures that do not match any other category
- **bridge**: the structure of the bridge
- **railtrack**: rail tracks that are non-drivable by cars
- **guardrail**: guard rails / crash barriers
- **traffic light**: traffic light boxes without their poles.

- **static**: elements in the scene and props that are immovable.
- **dynamic**: elements whose position is susceptible to change over time.
- **water**: horizontal water surfaces
- **terrain**: grass, ground-level vegetation, soil or sand
- **rider**: humans that ride/drive any kind of vehicle or mobility system
- **bicycle**: bicycles in scenes
- **motorcycle**: motorcycles in scene
- **bus**: buses in scenes
- **truck**: trucks in scenes

B.3 Depth & Instance Segmentation

We also provide depth and instance segmentation annotations along with semantic segmentation annotations. Both the depth and instance segmentation sensors are mounted alongside the RGB camera and semantic segmentation sensors. Depth is stored in the *LogarithmicDepth* format which provides better results for closer objects. We also provide depth-aided semantic segmentation results (training details in Sec. C.4).

B.4 SKYSCENES vs Real Characteristics

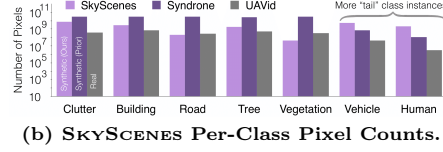
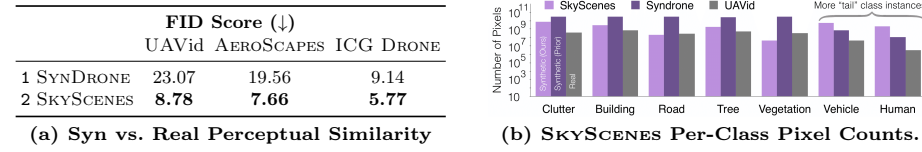


Fig. 7: SKYSCENES vs Real Characteristics. (a) Comparing perceptual similarity using FID scores calculated between real datasets (UAVid, AEROSCAPES, ICG DRONE) and synthetic datasets (SYNDROME, SKYSCENES). (b) We compare the number of densely annotated pixels per-class for SKYSCENES (ours), Syndrone (another synthetic aerial dataset), and UAVid (real aerial dataset). We can see how compared to both synthetic and real counterparts, SKYSCENES provides better representation of tail classes (vehicles, humans).

In Fig. 7a, we compare perceptual similarity (in terms of FID [15]) of synthetic images from SKYSCENES and SYNDROME [42] with real datasets (UAVid [27], AEROSCAPES [34], ICG DRONE [20]). We find SKYSCENES images are closer to real data distributions than SYNDROME [42]. For semantic comparisons, we show class-distribution comparisons (per-class pixel frequencies) between SKYSCENES, SYNDROME [42] and UAVid [27] in Fig 7b. SKYSCENES images display higher distribution of tail classes(vehicles, humans) compared to SYNDROME [42], and shows better alignment with the real data distribution (UAVid [27]).

C Experiment Details

C.1 Class Merging Details

Syn → UAVid	UAVid	SKYSCENES	SYNDRONE	VALID	SYNTHAER	Common Scheme	UAVid	AEROSCapes	ICG	DRONE	SKYSCENES
	clutter	unlabelled	unlabelled	background	sky	clutter	background	unlabeled	unlabeled	unlabeled	unlabeled
		sidewalk	sidewalk	pavement	footpath		sky	dirt	sky	sky	sky
		fence	fence	fence				grass	pole		
		bridge	bridge	bridge				gravel	sidewalk		
		water	water	water				water	traffic sign		
		traffic light	traffic light	traffic light				pool	other		
		other	other	sign				rock	ground		
		traffic sign	traffic sign	land				fence-pole	guard rail		
		rail track	rail track	tunnel				dog	traffic light		
		guard rail	guard rail	pool				ar-marker	static		
		static	static	stones				obstacle	dynamic		
1 clutter		dynamic	dynamic	pierrable				conflicting	water		
		ground	ground	chair					terrain		
		sky	sky	ice							
		pole	pole	ship							
				plane							
				harbor							
				lamp							
				bus stop							
				powerline							
				garbage bin							
				other low obstacle							
				other high obstacle							
2 building	building	building	wall	building	wall	building	building	wall	wall	wall	wall
3 road	road	road	roadline	road	roadline	road	road	road	road	road	road
4 vegetation	vegetation	vegetation	vegetation	tree	tree	vegetation	vegetation	tree	tree	tree	tree
5 low vegetation	terrain	terrain	terrain	other plant	vegetation	bald tree	bald tree	bald tree	bald tree	bald tree	bald tree
6 person	person	pedestrian	pedestrian	person		human	person	person	pedestrian	pedestrian	pedestrian
		rider	rider				bicycle	bicycle	bicycle	bicycle	bicycle
		motorcycle	motorcycle						rider	rider	rider
		bicycle	bicycle						motorcycle	motorcycle	motorcycle
7 vehicle	car	car	car	small vehicle	car	car	car	car	car	car	car
		truck	truck	large vehicle					truck	truck	truck
		bus	bus						bus	bus	bus

Table 7: Class merging scheme for **Table 8: Common class merging scheme across all real datasets and** evaluating Syn → UAVid experiments. The first column is the final set of merged classes we use for Syn → UAVid evaluation, the second column is the original UAVid [27] classes, the third column is the original SKYSCENES classes, the fourth column is the original AEROSCapes [34] classes, the fifth column is the original SYNTHAER [47] classes. Each row indicates all the classes from all the classes from UAVid, SKYSCENES, UAVid, AEROSCapes, ICG Drone, and SYNDRONE [42], VALID [5], and SYNTHAER [47] that were merged and correspond to the final Syn → UAVid class in the first column

Syn → AEROSCapes AEROSCapes SKYScenes SYDrone				SYn	→ ICG	Drone	ICG	Drone	SYKScenes	SYDrone	VALID	SYNTHAE
1 background	background	unlabelled	unlabelled	obstacle	unlabelled	unlabelled	background	animal	sky	sky		
	drone	other	other	dog	other	other	background	animal	sign	sign		
	boat	traffic sign	traffic sign	conflicting	traffic sign	traffic sign	background	ice	ice	ice		
	animal	rail track	rail track	ar-marker	sky	sky	background	trees	trees	trees		
	obstacle	guard rail	guard rail	unlabelled	bridge	bridge	background	traffic light	traffic light	traffic light		
		traffic light	traffic light		guard rail	guard rail	background	static	static	pierrable		
		static	static		traffic light	traffic light	background	dynamic	dynamic	garbage bin		
		dynamic	dynamic		static	static	background			plane		
		ground	ground				background			harbor		
		sidewalk	sidewalk				background			land		
2 bicycle	terrain	terrain	terrain				background			chair		
	water	water	water				background			ship		
	pole	pole	pole				background			lump		
							background			tunnel		
							background			bus stop		
3 person	bike	bicycle	bicycle	2 fence	fence	fence	background			bus stop		
		motorcycle	motorcycle	3 pole	fence pole	pole	background			powerline		
	person	pedestrian	pedestrian	4 vegetation	tree	vegetation	background			garbage bin		
		rider	rider	5 building	bald-tree	vegetation	background			other low obstacle		
4 vehicle	car	car	car	6 water	wall	wall	background			other high obstacle		
		truck	truck	7 bicycle	roof	building	background					
		bus	bus	8 vehicle	door	building	background					
		bus	train	9 person	window	building	background					
		train		10 paved area			background					
5 vegetation	vegetation	vegetation	vegetation	11 terrain			background					
							background					
							background					
							background					
6 building	construction	building	building				background					
		wall	wall				background					
		fence	fence				background					
		bridge	bridge				background					
7 road	road	road	road				background					
		roadline	roadline				background					
							background					
8 sky							background					
9							background					
10							background					
11							background					

Table 9: Class merging scheme for evaluating $\text{Syn} \rightarrow \text{AEROSCAPES}$ experiments The first column is the final set of merged classes we use for $\text{Syn} \rightarrow \text{AEROSCAPES}$ evaluation, the second column is the original **AEROSCAPES** [34] classes, the third column is the original **SKYSCENES** classes and the last column is the original **SYNDRONE** [42] classes. Each row indicates all the classes from **AEROSCAPES**, **SKYSCENES**, and **SYNDRONE** that were merged and correspond to the final $\text{Syn} \rightarrow \text{AEROSCAPES}$ class in the first column

► **Synthetic→Real.** As noted in Sec.4 of the main paper, since different real-world datasets have different class vocabularies and definitions, for our Synthetic → Real semantic segmentation experiments, we adapt the class-vocabulary of the synthetic source dataset (SKYSCENES, SYNDRONE, VALID, SYNTHAER) to that of the target real dataset (UAVid, AEROSCapes, ICG DRONE). This is done using a class-merging scheme based on the class-vocabularies and after visually inspecting dataset annotations. We provide the class-merging schemes used for the synthetic datasets (SKYSCENES, SYNDRONE [42], VALID [5] and SYNTHAER [47]) across real counterparts UAVid [27] (in Table. 7), AEROSCapes [34]

(in Table. 9) and ICG DRONE [20] (in Table. 10). We also include a coarser common merging scheme for SKYSCENES and all the real datasets UAVid, AEROSCAPES, and ICG DRONE in Table. 8.

▷ **SKYSCENES Diagnostic Experiments.** To assess the sensitivity of trained models to different factors – weather, time of day, height, pitch, *etc.* – we train models on different SKYSCENES variations and evaluate them on held-out-variations. For these experiments, we reduce the SKYSCENES vocabulary to a reasonable subset of 20 classes (consistent with the widely used Cityscapes [8] palette) – road, sidewalk, building, wall, fence, pole, traffic light, traffic sign, vegetation, water, sky, pedestrian, rider, cars, truck, bus, roadline, motorcycle, bicycle and an ignore class.

C.2 Training, Validation and Test Splits

SKYSCENES. For each (h, θ) combination, SKYSCENES has a total of 2800 data points (frames) which are distributed evenly across each of the 8 town layouts and 5 weather and daytime conditions. We use 80% (2240 images) of these data points for training models, and remaining 10% (280 images) each for validation and testing. While creating train, val and test splits, we collect equal number of samples from each town by dividing each town-specific traversal sequence into 3 segments: the initial 80% for training, the next 10% for testing, and the final 10% of the segment for validation. Moreover, within each split, we ensure that every viewpoint is accompanied by its 60 different variations across weather, daytime, height, and pitch settings. This safeguards against any potential cross-contamination across different splits while ensuring fair representation and equal distributions of all variations.

SYNDRONE. SYNDRONE has 3000 images per town (across 8 CARLA towns) for each of the 3 (h, θ) combinations, resulting in a total of $3000 \times 8 = 24,000$ images per (h, θ) combination. We use 20,000 of these data points for training models, with 4000 kept aside for testing. The data points selected for training and testing are kept consistent with the one reported in SYNDRONE [42].

VALID. VALID has a total of 6690 images spread across 3 different height variations and 6 different layout and daytime conditions all from the nadir perspective. For the 3 (h, θ) combination, $(h = 100m, \theta = 90^\circ)$, $(h = 50m, \theta = 90^\circ)$ and $(h = 20m, \theta = 90^\circ)$, the total images are 1734, 2158 and 2798 respectively which are split into 80% for training and 10% each for validation and testing. The data points selected for training and testing are kept consistent with the one reported in VALID [5].

SYNTHAER. The split of the dataset and the data points selected for training and testing are consistent with the one reported in SYNTHAER [47] with 435 images for training, 132 for validation and 198 for testing.

C.3 SKYSCENES Diagnostic Experiments

Weather & Daytime Variations. For each weather variation we sample evenly across the 8 towns and 9 (h, θ) combinations (excluding $\theta = 0^\circ$), re-

sulting in a total of $70 \times 9 \times 8 = 5040$ images. We use 80% (4032 images) of these for training models, and remaining 10% (504 images) each for validation and testing. We evaluate the model on the same weather variation it was trained on and select the model with the best mIoU score for further evaluations on other weather variations.

Town Variations. For each variation in town we sample evenly across 5 weather and daytime conditions and 9 height and pitch variations(excluding pitch=0° variations), resulting in a total of $70 \times 5 \times 9 = 3150$ images per town variation. Out of these, 80% (2520 images) is allocated for training models, with 10% (315 images) each for validation and testing. We evaluate the model on the same town variation it was trained on and select the model with the best mIoU score for further evaluations on other town variations.

Height & Pitch Variations. For each (h, θ) variation, we evenly sample across 8 towns and 5 weather and daytime conditions, resulting in a total of $70 \times 8 \times 5 = 2800$ images per height and pitch variation. Out of these, 80% (2240 images) are allocated for training models, and 10% (280 images) each for validation and testing. We evaluate the model on the same height & pitch setting it was trained on and select the model with the best mIoU score for further evaluations on other height & pitch settings.

C.4 Training Details

Semantic Segmentation. For our semantic segmentation experiments we use both CNN – DeepLabv2 [4] (ResNet-101 [14] backbone) – and vision transformer – 1. DAFormer [16] (with HRDA [17] source training; MiT-B5 [55] backbone) and 2. Rein DINOv2 [54] – based semantic segmentation architectures. Note that we utilize only the DAFormer architecture to perform source-only training for our experiments. Following [18], we enable rare class sampling [16] and use Imagenet feature-distance for our thing classes during training. DeepLabv2 [4] and DAFormer [16] are trained using the AdamW [26] optimizer coupled with a polynomial learning rate scheduler with an initial learning rate of 6×10^{-5} . For our fine-tuning experiments, we use an initial learning rate of 6×10^{-6} . For Rein [54], we use initial learning rate of 3×10^{-5} and for fine-tuning we use 3×10^{-6} . Each model is trained for 40k iterations with a batch size of 4.

Depth-Aided Semantic Segmentation. For our depth-aided semantic segmentation experiments in Sec. 4.3 of the main paper, similar to DAFormer [16], we employ a SegFormer [55] equivalent version of M3L [28] (multimodal segmentation network) with an MiT-B5 [55] backbone. We initialize the network with ImageNet-1k pre-trained checkpoints. For M3L Linear Fusion, we use $\alpha = 0.8$. We use AdamW [22] optimizer and train on a batch size of 4 for 50 epochs. We use a learning rate of 10^{-4} for the encoder and 3×10^{-4} for the decoder with a momentum of 0.9 and weight decay of 10^{-4} . We set the polynomial decay of power 0.9. We train both RGB and RGB+D models with complete supervision for $(h = 35m, \theta = 45^\circ)$ (moderate viewpoint) conditions on SKYSCENES.

C.5 Evaluation Details

Due to memory constraints, in addition to heavily parameterized models, our GPUs were unable to fit images larger than 1280×720 . Hence for high-resolution datasets like UAVid, we use the trained model to make separate predictions on 4 equally sized slightly-overlapping crops (overlap of 20 pixels) of the real image and stitch crop predictions to obtain the overall image prediction. Similarly, for ICG DRONE, we obtain overall image prediction using such crop predictions.

D Results

D.1 Ground vs Aerial Performance Gap

Recent advancements in synthetic-to-real (syn-to-real) generalization have significantly closed the performance gap in ground imagery to about **20%**, unlike in aerial imagery where the gap remains as high as **50%**. In our study, we evaluated Rein DINOv2 [54] across ground-view settings using GTAV → Cityscapes and aerial-view settings using SKYSCENES → ICG. For ground views, the gap between GTAV → Cityscapes and Cityscapes [8] mIoU was **16.29%**, demonstrating a mIoU of 66.7 compared to 82.99. Aerial views showed a larger gap, with SKYSCENES → ICG mIoU at 25.91 versus ICG mIoU at 76.44, resulting in a **50.53%** gap. This highlights the need for focused efforts to address the larger performance discrepancies observed in aerial imagery.

D.2 Advantage of SKYSCENES over Real Datasets

Curating densely annotated real data under diverse conditions in a controlled / uncontrolled manner is prohibitively expensive. As a synthetic alternative, SKYSCENES is well-suited for evaluating model sensitivity to changing conditions. Further, due to the lack of diverse annotated data, we observe that real aerial datasets are somewhat homogenous. Consequently, models trained on real data under specific conditions (unlike SKYSCENES) struggle to generalize to differing conditions – Rein DINOv2 [54] models trained on SKYSCENES generalize better to ICG DRONE [20] (64.15 mIoU) compared to ones trained on AEROSCAPES [34] (28.29 mIoU) and UAVid [27] (45.57 mIoU)⁶

D.3 Synthetic→Real Aligned Data Selection

As stated in the main paper, for our Synthetic→Real experiments, we train models on (h, θ) subsets of synthetic datasets that are aligned with corresponding real data (h, θ) conditions. In case of UAVid and AEROSCAPES we find that $(h = 35m, \theta = 45^\circ)$ viewpoints in SKYSCENES and $(h = 20m, \theta = 30^\circ)$ viewpoints in SYNDRONE are best aligned with UAVid conditions (see Table. 11 and Table. 12)

⁶ A common merging scheme was used as detailed in Table. 8

$h(\text{m})$	$\theta(\text{°})$	Synthetic \rightarrow UAVid mIoU (\uparrow)							
		Clutter	Building	Road	Tree	Low Vegetation	Human	Vehicle	Avg
SKYSCENES									
1 15	0	30.23	70.24	43.91	52.20	6.24	10.33	43.45	36.66
2 15	45	23.36	61.88	43.10	38.18	11.79	0.32	3.76	26.05
3 15	60	22.15	57.85	39.31	38.43	5.35	0.27	3.72	23.35
4 15	90	27.01	68.40	41.92	53.79	17.95	17.26	42.80	38.45
5 35	0	31.66	72.37	38.65	45.73	12.97	0.45	23.63	32.21
6 35	45	36.44	81.3	52.09	60.00	25.96	10.21	63.64	47.09
7 35	60	28.17	68.31	44.96	44.84	15.32	0.05	8.81	30.06
8 35	90	28.88	76.49	48.11	57.88	13.61	7.98	49.32	40.07
9 60	0	24.83	66.37	26.18	39.58	11.43	0.01	4.76	24.74
10 60	45	27.32	66.02	38.29	41.45	11.72	0.0	5.25	27.15
11 60	60	23.98	62.62	32.72	41.00	17.55	0.00	6.34	26.32
12 60	90	28.84	75.03	40.72	54.27	13.02	1.16	49.48	37.50
SYNDRONE									
13 20	30	36.20	75.74	48.71	55.95	28.75	8.27	42.52	42.31
14 50	60	31.13	69.93	48.87	54.49	27.71	1.32	36.06	38.50
15 80	90	28.89	65.66	42.05	51.51	32.16	0.13	28.39	35.54

Table 11: Models trained on UAVid aligned (h, θ) display better generalization performance. We have trained both SKYSCENES and SYNDRONE on every subset of (h, θ) provided by the respective datasets

$h(\text{m})$	$\theta(\text{°})$	Synthetic \rightarrow AEROSCAPES mIoU (\uparrow)							
		Background	Bicycle	Person	Vehicle	Vegetation	Building	Road	Sky
SKYSCENES									
1 15	0	32.39	0.00	3.45	55.42	56.08	30.11	15.4	69.75
2 15	45	25.26	0.0	4.12	5.72	31.9	11.56	26.43	7.23
3 15	60	27.16	0.00	1.69	11.81	32.27	22.48	31.22	0.21
4 15	90	28.53	1.32	30.35	77.22	53.09	12.09	11.43	0.00
5 35	0	32.45	0.00	0.00	17.65	51.00	42.03	7.14	75.03
6 35	45	32.07	0.8	3.09	80.99	51.34	45.54	23.64	88.29
7 35	60	29.72	0.00	0.00	30.00	45.54	24.01	23.26	0.00
8 35	90	30.62	1.9	2.62	72.77	55.56	26.85	17.34	1.94
9 60	0	29.99	0.0	0.0	1.05	34.68	42.11	10.53	49.63
10 60	45	28.05	0.0	0.0	7.14	40.60	22.38	17.84	5.16
11 60	60	26.71	0.0	0.0	0.53	37.93	19.95	18.63	0.80
12 60	90	31.08	0.00	0.11	30.83	58.10	31.61	17.76	0.06
SYNDRONE									
13 20	30	32.32	0.92	0.77	49.77	54.42	35.71	6.89	63.45
14 50	60	32.29	0.99	0.05	29.41	56.47	39.59	22.15	5.36
15 80	90	30.40	0.09	0.01	27.09	51.04	39.20	27.32	0.17

Table 12: Models trained on AEROSCAPES aligned (h, θ) display better generalization performance. We have trained both SKYSCENES and SYNDRONE on every subset of (h, θ) provided by the respective datasets

h (m)	θ (°)	Synthetic \rightarrow ICG DRONE mIoU (↑)												
		other	fence	pole	vegetation	building	water	bicycle	vehicle	person	paved area	terrain	Avg	Avg*
SKYSCENES														
1 15	0	2.85	0.28	0.04	6.60	29.94	0.83	0.06	0.45	0.35	27.46	0.72	6.33	7.33
2 15	45	2.87	0.67	0.21	6.91	32.12	3.25	0.49	5.03	25.22	56.69	8.78	12.93	14.51
3 15	60	3.98	0.00	0.73	5.19	35.85	0.66	0.12	4.95	3.56	57.51	1.21	10.34	12.06
4 15	90	3.74	1.45	2.51	6.67	46.72	8.19	2.21	39.71	45.89	79.84	6.04	22.09	25.91
5 35	0	1.63	0.00	0.06	4.86	28.84	2.77	0.07	0.04	0.30	29.70	6.96	6.84	7.40
6 35	45	4.37	0.39	1.60	4.90	25.33	4.98	0.10	1.35	0.29	68.37	29.51	12.83	11.92
7 35	60	2.06	0.01	0.04	6.15	30.05	9.43	0.02	0.23	0.11	54.99	13.43	10.59	11.23
8 35	90	2.13	0.04	0.64	7.34	28.07	7.26	0.09	0.30	0.11	50.27	11.11	9.76	9.63
9 60	0	2.23	0.00	0.00	8.30	32.07	1.72	0.10	0.03	0.17	11.58	13.30	6.32	6.00
10 60	45	1.07	0.00	0.02	7.71	30.03	4.73	0.17	0.00	0.22	31.62	8.87	7.68	8.28
11 60	60	0.81	0.00	0.02	4.84	26.59	7.21	0.16	0.01	0.16	51.34	8.39	9.05	9.11
12 60	90	1.32	0.00	0.25	7.90	27.64	3.21	0.04	0.26	0.22	21.36	6.65	6.26	6.76
SYNDRONE														
13 20	30	6.50	0.10	1.47	5.47	27.68	16.07	0.29	11.89	0.30	62.47	32.97	15.02	13.97
14 50	60	5.88	0.05	0.45	4.70	36.85	31.48	0.09	0.38	0.44	64.83	29.13	15.84	15.47
15 80	90	4.17	0.01	0.25	0.67	37.34	36.11	0.04	0.24	0.38	68.21	41.85	17.75	15.92

Table 13: Models trained on ICG DRONE aligned (h, θ) display better generalization performance. We have trained both SKYSCENES and SYNDRONE on every subset of (h, θ) provided by the respective datasets. Avg* - Average IoU reported over all classes excluding *other* and *terrain* (both numbers are reported since a discrepancy was observed in other and terrain class from SKYSCENES which resulted in overlapping cases across these classes)

and provide best transfer performance. Similarly, for ICG DRONE we observe that $(h = 15m, \theta = 90^\circ)$ SKYSCENES conditions are best aligned with the low-altitude, nadir perspective imagery in ICG DRONE and lead to best transfer performance (see Table. 13). However, for SYNDRONE, we find that the model trained on $(h = 80m, \theta = 90^\circ)$ has best transfer performance, indicating that model performance is more sensitive to pitch alignment than height alignment.

D.4 Synthetic \rightarrow Real Additional Experiments

(Source)	(Target)	Real-World mIoU (↑)
Synthetic	UAVid AEROSCAPES	ICG DRONE
1 SYNTHAER	39.56	29.69
2 VALID	45.03	32.80
3 SYNDRONE	54.92	40.28
4 SKYSCENES	54.19	43.96
		28.10

Table 14: Syn \rightarrow Real Rein Semantic Segmentation

A proper comparison with other synthetic datasets on a recognition task would require similar classes, (which a subset of synthetic alternatives, such as MidAir [12],

do not satisfy). Considering other desired attributes (outlined in Table.1 in the paper), we chose SYNDROME [42] as the most aligned alternative for our experiments. For comprehensive analysis and additional comparisons with other synthetic alternatives across various Synthetic→Real settings, we included comparisons with VALID [5], which features only nadir perspective, and SYNTHERAER [47], which lacks human classes, in Table 14. From the results in Table 14 , it is evident that models trained on SKYSCENES generalize better to real datasets compared to other synthetic alternatives.

D.5 SKYSCENES + Real Data Experiments

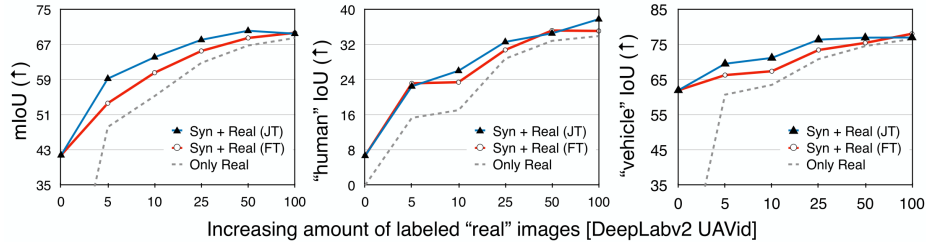


Fig. 8: [DeepLabv2 UAVid] SKYSCENES can augment “real” training data. We show how SKYSCENES can additionally augment real (UAVid [27]) training data. We compare DeepLabv2 [4] models trained using only 5%, 10%, 25%, 50%, 100% of labeled UAVid [27] images with counterparts that were either (1) pretrained on SKYSCENES, and finetuned on UAVid [27] (FT) or (2) trained jointly on SKYSCENES and UAVid [27] (JT). We find that [Left] additionally augmenting training data with SKYSCENES and help improve real-world generalization in low-shot regimes, [Middle, Right] especially for under-represented classes.

In addition to zero-shot transfer to real data, we also show how SKYSCENES is useful as additional training data when labeled real-world data is available. In Fig. 8 and Fig. 9, we compare the performance of DeepLabv2 [4] for SKYSCENES →UAVid [27] and for SKYSCENES →AEROSCapes [34] trained only using 5%, 10%, 25%, 50%, 100% of UAVid [27] and AEROSCapes [34] training images respectively with counterparts that were either pretrained using SKYSCENES data or additionally supplemented with SKYSCENES data at training time. In Fig. 10 and Fig. 11 we make a similar comparison with the DAFormer [16] architecture, and in Fig. 12 with the Rein DINOv2 [54] architecture. In low-shot regimes (when little “real” world data is available), SKYSCENES data (either explicitly via joint training or implicitly via finetuning) is beneficial in improving recognition performance. We find this to be especially beneficial for under-represented classes in aerial imagery (such as `humans` and `vehicles`). In Table. 15 and Table. 16 we present similar fine-grained (per-class) comparison of SKYSCENES with SYNDROME for a DeepLabv2 model when real data is available for training

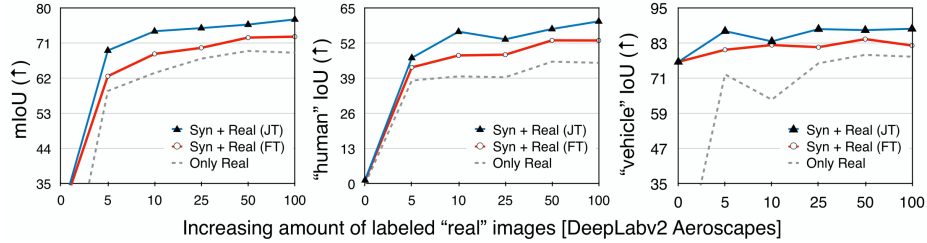


Fig. 9: [DeepLabv2 Aeroscapes] SKYSCENES can augment “real” training data. We show how SKYSCENES can additionally augment real (Aeroscapes [34]) training data. We compare DeepLabv2 [4] models trained using only 5%, 10%, 25%, 50%, 100% of labeled Aeroscapes [34] images with counterparts that were either (1) pretrained on SKYSCENES, and finetuned on Aeroscapes [34] (FT) or (2) trained jointly on SKYSCENES and Aeroscapes [34] (JT). We find that [Left] additionally augmenting training data with SKYSCENES and help improve real-world generalization in low-shot regimes, [Middle, Right] especially for under-represented classes.

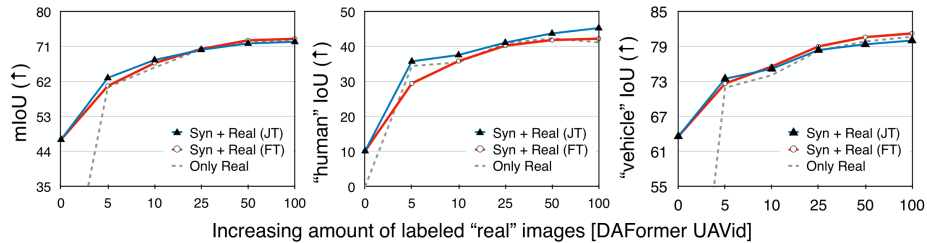


Fig. 10: [DAFormer UAVid] SKYSCENES can augment “real” training data. We show how SKYSCENES can additionally augment real (UAVid [27]) training data. We compare DAFormer [16] models trained using only 5%, 10%, 25%, 50%, 100% of labeled UAVid [27] images with counterparts that were either (1) pretrained on SKYSCENES, and finetuned on UAVid [27] (FT) or (2) trained jointly on SKYSCENES and UAVid [27] (JT). We find that [Left] additionally augmenting training data with SKYSCENES and help improve real-world generalization in low-shot regimes, [Middle, Right] especially for under-represented classes.

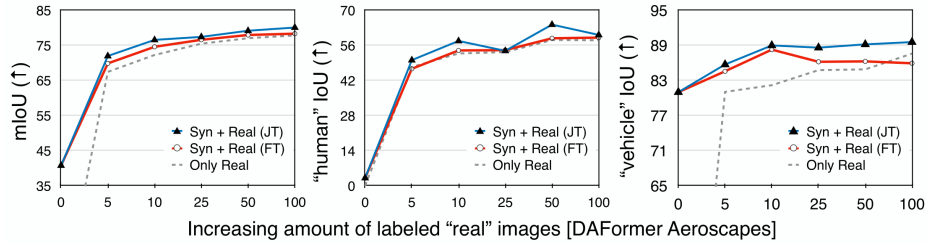


Fig. 11: [DAFormer Aeroscapes] SKYSCENES can augment “real” training data. We show how SKYSCENES can additionally augment real (Aeroscapes [34]) training data. We compare DAFormer [16] models trained using only 5%, 10%, 25%, 50%, 100% of labeled Aeroscapes [34] images with counterparts that were either (1) pretrained on SKYSCENES, and finetuned on Aeroscapes [34] (FT) or (2) trained jointly on SKYSCENES and Aeroscapes [34] (JT). We find that [Left] additionally augmenting training data with SKYSCENES and help improve real-world generalization in low-shot regimes, [Middle, Right] especially for under-represented classes.

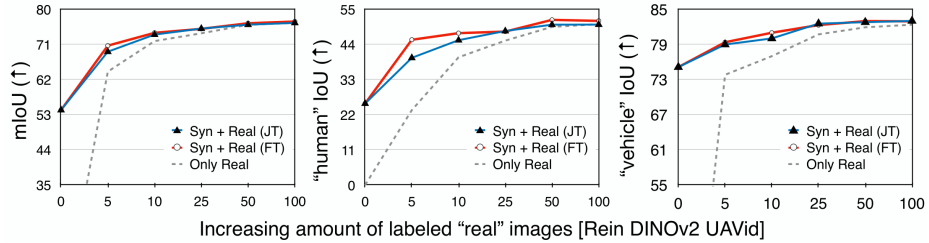


Fig. 12: [Rein DINOv2 UAVid] SKYSCENES can augment “real” training data. We show how SKYSCENES can additionally augment real (UAVid [27]) training data. We compare Rein DINOv2 [54] models trained using only 5%, 10%, 25%, 50%, 100% of labeled UAVid [27] images with counterparts that were either (1) pretrained on SKYSCENES, and finetuned on UAVid [27] (FT) or (2) trained jointly on SKYSCENES and UAVid [27] (JT). We find that [Left] additionally augmenting training data with SKYSCENES and help improve real-world generalization in low-shot regimes, [Middle, Right] especially for under-represented classes.

Training	Data Size	Synthetic \rightarrow UAVid mIoU (\uparrow)							
		Clutter	Building	Road	Tree	Low Vegetation	Human	Vehicle	Avg
SKYSCENES									
1 FT	5%	47.60	83.73	62.08	58.98	33.70	23.21	66.36	53.67
2 FT	10%	50.06	86.93	67.70	70.58	58.09	23.47	67.46	60.61
3 FT	25%	57.61	89.37	73.28	73.30	61.15	30.82	73.50	65.57
4 FT	50%	62.44	90.87	75.84	74.75	65.16	35.24	75.52	68.54
5 FT	100%	63.56	91.23	77.03	76.01	66.81	35.14	78.12	69.70
6 JT	5%	52.09	86.83	65.35	68.45	50.06	22.53	69.59	59.27
7 JT	10%	56.23	89.06	71.84	73.23	61.35	26.07	71.25	64.15
8 JT	25%	61.50	90.45	75.98	75.18	64.56	32.65	76.45	68.11
9 JT	50%	65.70	91.68	78.14	76.84	67.29	34.59	77.02	70.18
10 JT	100%	64.19	89.06	74.52	76.59	67.34	37.82	77.06	<u>69.51</u>
SYNDRONE									
11 FT	5%	46.58	82.81	59.69	58.95	37.53	21.50	63.78	52.97
12 FT	10%	48.08	85.76	64.56	69.14	54.29	21.91	65.94	58.53
13 FT	25%	56.46	88.78	70.97	72.06	61.14	28.59	73.12	64.45
14 FT	50%	61.70	90.45	73.83	75.48	64.67	33.45	74.98	67.79
15 FT	100%	63.42	91.16	75.75	76.56	66.63	33.53	76.59	69.10
16 JT	5%	49.72	81.39	63.63	65.52	49.00	6.70	70.19	55.17
17 JT	10%	52.94	85.41	67.25	71.47	59.05	23.32	72.43	61.70
18 JT	25%	59.99	87.79	72.26	74.00	65.59	36.32	75.91	67.40
19 JT	50%	63.38	88.88	74.09	74.97	66.85	38.47	77.45	69.16
20 JT	100%	64.06	89.09	74.61	75.98	67.31	40.59	78.40	70.01
Target									
21 Target	5%	41.36	80.24	57.07	57.20	25.72	15.35	60.79	48.25
22 Target	10%	42.94	81.50	61.06	67.51	53.32	17.10	63.58	55.29
23 Target	25%	53.57	86.89	69.70	70.95	59.22	28.82	70.91	62.86
24 Target	50%	59.75	89.42	72.58	74.28	64.09	32.89	74.61	66.81
25 Target	100%	62.45	90.76	74.41	75.83	65.65	33.97	76.65	68.53

Table 15: [DeepLabv2 UAVid] SKYSCENES can augment “real” training data.

We compare SKYSCENES against SYNDRONE for their ability to additionally augment real (UAVid [27]) training data. We compare DeepLabv2 [4] models trained using only 5%, 10%, 25%, 50%, 100% of labeled UAVid [27] images with counterparts that were either (1) pretrained on SKYSCENES/SYNDRONE, and finetuned on UAVid [27] (FT) or (2) trained jointly on SKYSCENES/SYNDRONE and UAVid [27] (JT). We find that both FT and JT with SKYSCENES outperforms SYNDRONE in almost all of the different labeled data splits.

Training	Data Size	Synthetic \rightarrow AEROSCAPES mIoU (\uparrow)								
		Background	Bicycle	Person	Vehicle	Vegetation	Building	Road	Sky	Avg
SKYSCENES										
1 FT	5%	59.25	4.69	43.11	80.81	91.79	59.32	72.43	89.13	62.57
2 FT	10%	71.45	14.76	47.53	82.43	92.96	60.08	83.92	93.09	68.28
3 FT	25%	72.93	21.78	47.80	81.69	93.42	62.25	84.51	94.30	69.84
4 FT	50%	76.15	23.69	53.11	84.45	93.58	67.00	87.73	94.06	72.47
5 FT	100%	76.91	25.30	53.07	82.27	94.05	67.81	87.78	94.51	72.71
6 JT	5%	67.86	22.42	46.63	87.18	92.11	59.69	85.04	92.31	69.16
7 JT	10%	76.24	30.44	56.33	83.67	92.15	69.39	89.70	94.86	74.10
8 JT	25%	76.33	34.14	53.50	87.87	93.12	68.89	90.23	95.23	74.91
9 JT	50%	78.13	32.06	57.32	87.52	93.23	73.14	90.42	94.69	<u>75.81</u>
10 JT	100%	80.35	32.43	60.14	87.98	94.00	75.20	91.89	95.06	77.13
SYNDRONE										
11 FT	5%	57.20	3.79	39.07	77.44	90.79	58.60	69.09	88.48	60.56
12 FT	10%	69.18	14.77	47.07	64.87	92.29	60.42	81.09	91.94	65.20
13 FT	25%	72.21	23.27	44.35	79.72	92.83	63.94	83.31	92.31	68.99
14 FT	50%	74.28	22.32	49.59	81.59	93.01	64.70	85.56	92.81	70.49
15 FT	100%	74.61	22.45	49.13	81.42	93.15	64.18	86.15	92.64	70.47
16 JT	5%	63.05	23.34	46.50	83.30	92.24	64.15	78.81	93.64	68.12
17 JT	10%	74.54	26.14	53.81	81.26	93.01	66.44	88.83	94.62	72.32
18 JT	25%	76.96	33.69	55.34	83.53	93.67	69.00	90.37	95.26	74.73
19 JT	50%	79.35	31.45	59.18	85.80	93.66	74.00	91.27	95.05	76.22
20 JT	100%	79.66	31.82	58.71	86.87	93.75	74.65	91.95	94.20	76.45
Target										
21 Target	5%	53.92	7.33	38.25	72.41	90.15	53.49	66.79	87.95	58.79
22 Target	10%	67.08	14.89	39.79	63.76	91.65	58.98	79.45	91.70	63.41
23 Target	25%	70.51	20.69	39.46	76.20	92.34	62.25	82.51	92.56	67.07
24 Target	50%	73.10	20.95	45.23	79.07	92.68	64.70	84.48	92.11	69.04
25 Target	100%	73.21	19.21	44.79	78.44	92.95	63.49	85.34	91.27	68.59

Table 16: [DeepLabv2 Aeroscapes] SKYSCENES can augment “real” training data. We compare SKYSCENES against SYNDRONE for their ability to additionally augment real (Aeroscapes [34]) training data. We compare DeepLabv2 [4] models trained using only 5%, 10%, 25%, 50%, 100% of labeled Aeroscapes [34] images with counterparts that were either (1) pretrained on SKYSCENES/SYNDRONE, and finetuned on Aeroscapes [34] (FT) or (2) trained jointly on SKYSCENES/SYNDRONE and Aeroscapes [34] (JT). We find that both FT and JT with SKYSCENES outperforms SYNDRONE in almost all of the different labeled data splits.

Training	Data Size	Synthetic \rightarrow UAVid mIoU (\uparrow)							
		Clutter	Building	Road	Tree	Low Vegetation	Human	Vehicle	Avg
SKYSCENES									
1 FT	5%	52.63	88.02	67.74	66.56	49.14	29.53	72.68	60.90
2 FT	10%	57.43	89.48	72.93	74.26	61.96	35.89	75.61	66.79
3 FT	25%	63.43	90.87	78.66	75.59	64.94	40.29	79.05	70.41
4 FT	50%	67.06	92.22	79.76	77.86	68.97	41.90	80.64	72.63
5 FT	100%	67.67	92.51	79.66	78.68	69.03	42.29	81.27	73.02
6 JT	5%	53.72	85.99	66.35	69.02	56.45	35.82	73.51	62.97
7 JT	10%	59.77	87.82	72.97	74.68	64.95	37.63	75.21	67.58
8 JT	25%	63.58	88.68	76.22	75.80	67.49	41.17	78.43	70.20
9 JT	50%	66.83	89.63	77.76	76.90	68.45	43.79	79.41	71.83
10 JT	100%	66.92	89.74	76.89	77.98	68.81	45.32	80.06	72.25
SYNDRONE									
11 FT	5%	53.53	87.81	67.31	67.51	55.40	33.94	73.40	62.70
12 FT	10%	56.80	89.64	72.31	74.22	64.12	36.77	75.15	67.00
13 FT	25%	63.77	91.11	78.18	76.17	66.63	41.27	78.90	70.86
14 FT	50%	66.89	92.06	79.14	77.79	69.22	43.32	80.47	72.70
15 FT	100%	67.48	92.48	79.48	78.76	69.73	42.82	81.57	73.19
16 JT	5%	53.54	85.58	64.30	70.07	58.64	29.86	73.21	62.17
17 JT	10%	58.00	87.26	71.23	74.57	64.65	35.58	75.08	66.62
18 JT	25%	61.82	88.35	74.09	75.38	66.43	40.85	78.21	69.31
19 JT	50%	65.10	89.19	75.80	76.95	68.15	40.65	78.52	70.62
20 JT	100%	66.78	89.81	76.56	77.91	69.38	45.34	80.45	72.32
Target									
21 Target	5%	51.20	86.59	62.68	66.73	50.46	34.50	71.97	60.59
22 Target	10%	53.95	88.35	70.56	73.65	63.29	35.50	74.12	65.63
23 Target	25%	62.86	90.48	76.89	76.02	66.66	41.03	78.31	70.31
24 Target	50%	66.23	91.84	78.75	77.61	68.44	42.36	79.90	72.16
25 Target	100%	66.67	92.20	79.16	78.35	68.93	41.25	80.70	72.47

Table 17: [DAFormer UAVid] SKYSCENES can augment “real” training data.

We compare SKYSCENES against SYNDRONE for their ability to additionally augment real (UAVid [27]) training data. We compare DAFormer [16] models trained using only 5%, 10%, 25%, 50%, 100% of labeled UAVid [27] images with counterparts that were either (1) pretrained on SKYSCENES/SYNDRONE, and finetuned on UAVid [27] (FT) or (2) trained jointly on SKYSCENES/SYNDRONE and UAVid [27] (JT). We find that both FT and JT with SKYSCENES outperforms or is on par with SYNDRONE in almost all of the different labeled data splits.

Training	Data Size	Synthetic \rightarrow AEROSCAPES mIoU (\uparrow)								
		Background	Bicycle	Person	Vehicle	Vegetation	Building	Road	Sky	Avg
SKYSCENES										
1 FT	5%	66.93	28.05	46.63	84.56	93.29	64.03	79.76	95.41	69.83
2 FT	10%	76.11	31.60	53.95	88.26	93.92	67.90	88.45	96.25	74.56
3 FT	25%	79.68	39.95	54.07	86.18	94.22	71.31	91.53	95.66	76.56
4 FT	50%	81.09	39.03	58.80	86.25	94.42	76.20	91.15	96.45	77.93
5 FT	100%	81.78	41.22	59.06	85.93	94.62	76.06	91.47	96.40	78.31
6 JT	5%	69.98	33.78	50.09	85.72	93.94	64.09	82.32	95.64	71.94
7 JT	10%	78.47	38.45	57.73	88.98	94.39	67.87	90.23	96.14	76.53
8 JT	25%	81.07	40.95	53.79	88.60	94.30	71.92	92.76	95.77	77.39
9 JT	50%	81.55	39.43	64.25	89.16	94.30	76.81	91.34	96.30	79.14
10 JT	100%	83.13	44.90	60.14	89.55	94.93	79.55	92.49	95.83	80.06
SYNDRONE										
11 FT	5%	70.94	29.02	47.17	82.25	93.23	64.19	83.31	93.27	70.42
12 FT	10%	76.62	29.13	60.31	86.91	93.80	66.29	89.80	95.65	74.81
13 FT	25%	78.97	34.86	57.69	86.06	93.83	69.73	92.03	95.33	76.06
14 FT	50%	80.28	34.42	63.33	85.34	94.31	73.71	91.55	95.69	77.33
15 FT	100%	80.90	35.47	62.18	85.43	94.45	74.45	92.12	95.76	77.59
16 JT	5%	69.12	30.82	53.16	81.33	93.19	61.11	83.80	95.36	70.99
17 JT	10%	77.38	40.42	57.80	88.32	94.14	68.06	90.24	95.60	76.47
18 JT	25%	80.64	44.19	53.95	89.80	94.28	71.89	92.58	96.14	77.94
19 JT	50%	81.82	40.86	63.15	89.20	94.38	77.72	92.29	96.43	79.42
20 JT	100%	79.38	35.85	50.91	86.01	94.08	70.88	90.73	94.32	75.27
Target										
21 Target	5%	66.26	24.03	47.34	81.04	92.88	58.85	78.11	90.85	67.42
22 Target	10%	74.91	32.00	52.74	82.18	93.62	59.63	88.73	94.00	72.23
23 Target	25%	78.16	41.22	53.29	84.76	93.95	66.04	90.92	95.28	75.45
24 Target	50%	80.09	38.73	58.11	84.89	94.14	73.72	90.85	95.61	77.02
25 Target	100%	80.35	42.65	57.99	87.58	94.48	72.65	91.20	95.51	77.80

Table 18: [DAFormer Aeroscapes] SKYSCENES can augment “real” training data. We compare SKYSCENES against SYNDRONE for their ability to additionally augment real (Aeroscapes [34]) training data. We compare DAFormer [16] models trained using only 5%, 10%, 25%, 50%, 100% of labeled Aeroscapes [34] images with counterparts that were either (1) pretrained on SKYSCENES/SYNDRONE, and finetuned on Aeroscapes [34] (FT) or (2) trained jointly on SKYSCENES/SYNDRONE and Aeroscapes [34] (JT). We find that both FT and JT with SKYSCENES outperforms or is on par with SYNDRONE in almost all of the different labeled data splits.

Training	Data Size	Synthetic → UAVid mIoU (↑)							
		Clutter	Building	Road	Tree	Low Vegetation	Human	Vehicle	Avg
SKYSCENES									
1 FT	5%	61.91	91.38	77.16	74.79	64.8	45.49	79.39	70.7
2 FT	10%	67.41	92.21	81.14	78.79	69.82	47.56	81.01	73.99
3 FT	25%	69.32	93.39	83.75	78.88	69.4	48.05	82.32	75.01
4 FT	50%	71.37	93.57	84.15	80.14	71.14	51.72	83	76.44
5 FT	100%	72.96	94.06	84.33	80.63	71.89	51.4	82.96	76.89
6 JT	5%	61.47	90.65	76.46	73.78	62.87	39.83	79	69.15
7 JT	10%	67.55	92.12	82.54	78.21	68.94	45.36	80.04	73.54
8 JT	25%	69.07	93.41	83.34	79.07	69.89	48.23	82.57	75.08
9 JT	50%	71.1	93.5	84.11	79.9	70.9	50.22	82.81	76.08
10 JT	100%	72.16	93.93	84.14	80.32	71.99	50.24	83.03	76.54
Target									
21 Target	5%	58.19	89.25	71.01	71.86	60.65	23.46	73.83	64.04
22 Target	10%	66.39	92.22	80.62	78.11	68.78	40.00	77.01	71.87
23 Target	25%	68.57	93.14	82.59	78.34	68.52	45.22	80.73	73.87
24 Target	50%	71.52	93.93	84.27	80.07	71.12	49.53	81.94	76.05
25 Target	100%	72.38	93.98	84.63	80.63	71.52	50.36	82.38	76.55

Table 19: [Rein DINOv2 UAVid] SKYSCENES can augment “real” training data. We show SKYSCENES’s ability to additionally augment real (UAVid [27]) training data. We compare Rein DINOv2 [54] models trained using only 5%, 10%, 25%, 50%, 100% of labeled UAVid [27] images with counterparts that were either (1) pretrained on SKYSCENES, and finetuned on UAVid [27] (FT) or (2) trained jointly on SKYSCENES and UAVid [27] (JT). We find that both FT and JT with SKYSCENES improve the performance on Target only.

– via Target-Only, Finetuning or Joint-Training. Tables. 17 and 18 show similar comparisons using the DAFormer [16] model. Table. 19 shows similar comparison using the Rein DINOV2 [54] model.

D.6 SKYSCENES Diagnostic Experiments

Test mIoU (\uparrow) Pitch					Test mIoU (\uparrow) Pitch					Test mIoU (\uparrow) Pitch					Test mIoU (\uparrow) Pitch				
Height	$\theta = 0^\circ$	$\theta = 45^\circ$	$\theta = 60^\circ$	$\theta = 90^\circ$	Height	$\theta = 0^\circ$	$\theta = 45^\circ$	$\theta = 60^\circ$	$\theta = 90^\circ$	Height	$\theta = 0^\circ$	$\theta = 45^\circ$	$\theta = 60^\circ$	$\theta = 90^\circ$	Height	$\theta = 0^\circ$	$\theta = 45^\circ$	$\theta = 60^\circ$	$\theta = 90^\circ$
1 h = 15m	72.57	66.38	57	39.46	1 h = 15m	59.03	66.98	63.07	61.85	1 h = 15m	45.36	64.13	68.88	69.28	1 h = 15m	30.61	55.79	64.98	71.93
2 h = 35m	59.07	55.55	54.43	39.23	2 h = 35m	43.8	49.41	49.91	45.19	2 h = 35m	30.49	45.05	50.39	53.44	2 h = 35m	16.84	33.2	37.89	48.63
3 h = 60m	48.58	44.94	43.85	31.71	3 h = 60m	34.27	39.86	40.1	35.42	3 h = 60m	21.86	31.21	36.51	38.43	3 h = 60m	11.26	21.12	26.38	31.22
(a) Height 15 & Pitch 0°					(b) Height 15 & Pitch 45°					(c) Height 15 & Pitch 60°					(d) Height 15 & Pitch 90°				
Test mIoU (\uparrow) Pitch					Test mIoU (\uparrow) Pitch					Test mIoU (\uparrow) Pitch					Test mIoU (\uparrow) Pitch				
Height	$\theta = 0^\circ$	$\theta = 45^\circ$	$\theta = 60^\circ$	$\theta = 90^\circ$	Height	$\theta = 0^\circ$	$\theta = 45^\circ$	$\theta = 60^\circ$	$\theta = 90^\circ$	Height	$\theta = 0^\circ$	$\theta = 45^\circ$	$\theta = 60^\circ$	$\theta = 90^\circ$	Height	$\theta = 0^\circ$	$\theta = 45^\circ$	$\theta = 60^\circ$	$\theta = 90^\circ$
1 h = 15m	52.14	47.62	39.04	29.31	1 h = 15m	48.50	50.71	45.22	42.21	1 h = 15m	37.21	49.04	47.42	44.93	1 h = 15m	28.73	40.11	44.9	46
2 h = 35m	58.03	55.61	55.07	45.54	2 h = 35m	50.49	55.74	57.11	52.19	2 h = 35m	34.37	52.67	57.52	54.14	2 h = 35m	25.89	38.98	46.26	54.02
3 h = 60m	53.31	50.38	50.23	46.65	3 h = 60m	45.33	49.79	50.37	44.62	3 h = 60m	29.82	44.36	48.33	44.71	3 h = 60m	20.36	29.95	36.1	43.16
(e) Height 35 & Pitch 0°					(f) Height 35 & Pitch 45°					(g) Height 35 & Pitch 60°					(h) Height 35 & Pitch 90°				
Test mIoU (\uparrow) Pitch					Test mIoU (\uparrow) Pitch					Test mIoU (\uparrow) Pitch					Test mIoU (\uparrow) Pitch				
Height	$\theta = 0^\circ$	$\theta = 45^\circ$	$\theta = 60^\circ$	$\theta = 90^\circ$	Height	$\theta = 0^\circ$	$\theta = 45^\circ$	$\theta = 60^\circ$	$\theta = 90^\circ$	Height	$\theta = 0^\circ$	$\theta = 45^\circ$	$\theta = 60^\circ$	$\theta = 90^\circ$	Height	$\theta = 0^\circ$	$\theta = 45^\circ$	$\theta = 60^\circ$	$\theta = 90^\circ$
1 h = 15m	37.59	32.89	24.53	18.35	1 h = 15m	43.01	43.33	35.6	31.05	1 h = 15m	38.58	43.4	36.96	32.22	1 h = 15m	28.12	34.9	33.6	33.28
2 h = 35m	48.42	44.31	42.82	32.04	2 h = 35m	52.13	57.6	58.84	51.95	2 h = 35m	44.69	57.52	60.21	54.3	2 h = 35m	32.76	45.32	53.71	55.27
3 h = 60m	51.53	48.38	47.71	39.45	3 h = 60m	51.89	56.83	56.43	50.07	3 h = 60m	43.24	56.68	59.27	49.18	3 h = 60m	29.58	42.59	50.73	57.07
(i) Height 60 & Pitch 0°					(j) Height 60 & Pitch 45°					(k) Height 60 & Pitch 60°					(l) Height 60 & Pitch 90°				

Table 20: Model Sensitivity to changing Height and Pitch. We evaluate a model trained on one h, θ variation (indicated by sub-table caption) across all other h, θ variations. Performant conditions are highlighted in blue.

Similar to Table 6 (d) in the main paper, in Table 20, we assess broader (h, θ) sensitivity of models by training DAFormer [16] models across all (total 12) (h, θ) settings and evaluate them across the same conditions in SKYSCENES. Table 20 (a) models trained on $(h = 15m, \theta = 0^\circ)$ are representative of one extreme of the range (both lowest height and pitch values) – we notice that this model is *extremely sensitive* to height variations. Tables 20 (a), (e) and (i), we can deduce that due to the high variability in perspective between $\theta = 0^\circ$ and other $\theta \neq 0^\circ$ conditions, models trained on $\theta = 0^\circ$ do not generalize well to other θ values. On the other hand, Tables. 20 (b), (c), (d), (f), (g) and (h) models trained on oblique perspectives are better at generalizing to other pitch conditions.

D.7 Visual Artifacts

Real-world images can have sensory artifacts beyond weather/daytime variations (UAV123 [30], VIRAT [35], UG² [52]). Prior work (RobustNav [2]) shows it's

Daytime Conditions	Vanilla	Test mIoU (↑)			
		Motion Blur		Spatter	
		sev. = 3	sev. = 5	sev. = 3	sev. = 5
Noon	83.54	74.31 (9.23↓)	67.49 (16.05↓)	78.42 (5.11↓)	63.03 (20.51↓)
Sunset	84.32	74.62 (9.70↓)	68.08 (16.24↓)	78.10 (6.22↓)	68.62 (15.69↓)

(a) Degraded Performance of Rein models under Visual Corruptions.



(b) Simulating Visual Artifacts.

possible to simulate such corruptions with varying severities. Fig.13b provides examples of motion blur and spatter, highlighting how models trained on clean data degrade under these conditions (see Table. 13a).

D.8 Auto labeling for Real Datasets

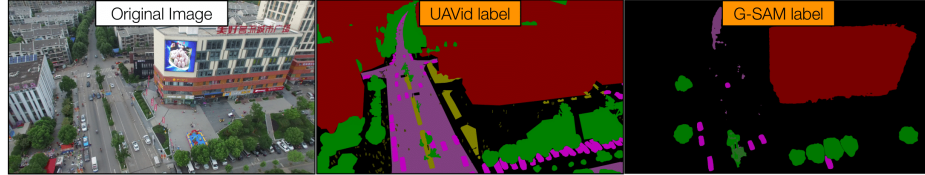


Fig. 14: Grounded-SAM predictions on a UAVid image.

Fig.14 shows a sample semantic segmentation prediction of a random UAVid image using Grounded-SAM [41]. We find that most of the roads are absent from the prediction, no humans are predicted, and only a few instances of vehicles, buildings, and trees are identified correctly. While auto-labeling using foundation models has potential, we believe there is still room for improvement in specific applications (such as aerial).

D.9 Qualitative examples

In Fig. 15, 16 and 17, we show qualitative examples of predictions made by SKYSCENES and SYNDRONE trained DeepLabv2 and DAFormer models on UAVid,

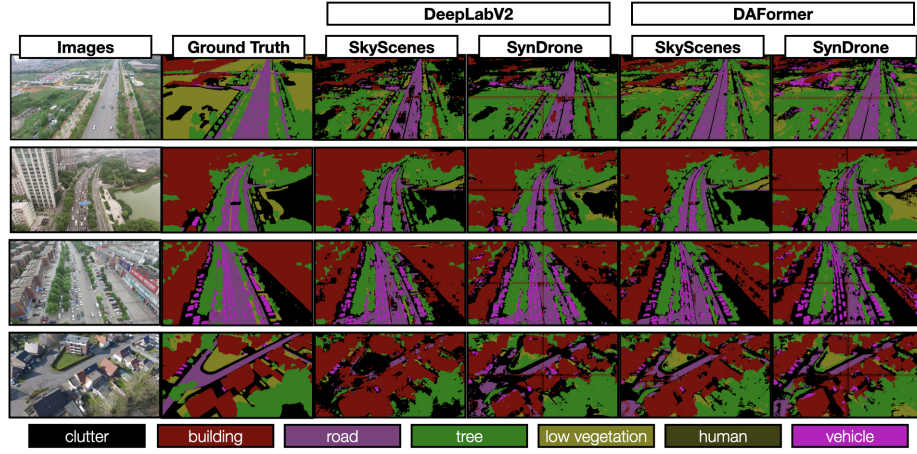


Fig. 15: Synthetic → UAVid Semantic Segmentation Predictions Out-of-the-box semantic segmentation predictions made on randomly selected UAVid [27] validation images by models trained on SKYSCENES and SYNDRONE. The first two columns indicate the original image and the associated ground truth respectively, columns 3 (SKYSCENES) and 4 (SYNDRONE) indicate predictions by DeepLabv2 [4] models and columns 5 (SKYSCENES) and 6 (SYNDRONE) indicate predictions made by DAFormer [16] models.

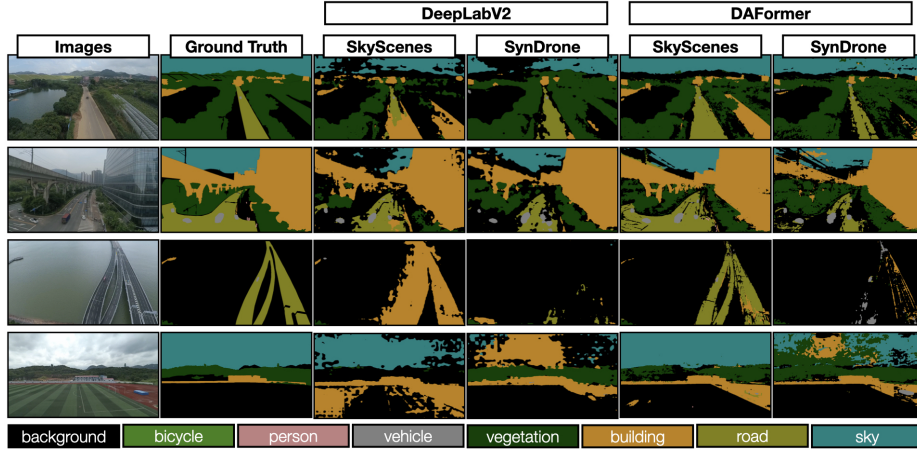


Fig. 16: Synthetic → AEROSCapes Out of the box semantic Segmentation Predictions Out-of-the-box semantic segmentation predictions made on randomly selected AEROSCapes [34] validation images by models trained on SKYSCENES and SYNDRONE. The first two columns indicate the original image and the associated ground truth respectively, columns 3 (SKYSCENES) and 4 (SYNDRONE) indicate predictions by DeepLabv2 [4] models and columns 5 (SKYSCENES) and 6 (SYNDRONE) indicate predictions made by DAFormer [16] models.

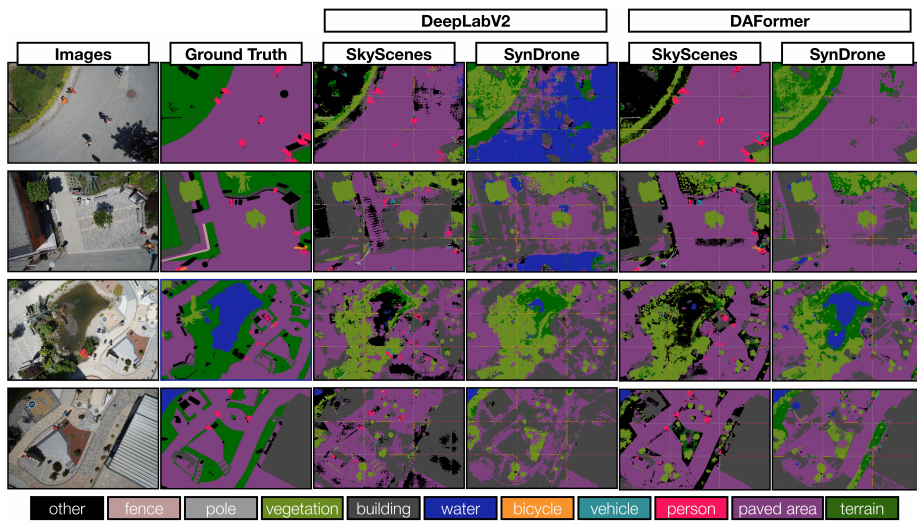


Fig. 17: Synthetic → ICG DRONE Out of the box semantic Segmentation Predictions Out-of-the-box semantic segmentation predictions made on randomly selected ICG DRONE [20] validation images by models trained on SKYSCENES and SYNDRONE. The first two columns indicate the original image and the associated ground truth respectively, columns 3 (SKYSCENES) and 4 (SYNDRONE) indicate predictions by DeepLabv2 [4] models and columns 5 (SKYSCENES) and 6 (SYNDRONE) indicate predictions made by DAFormer [16] models.

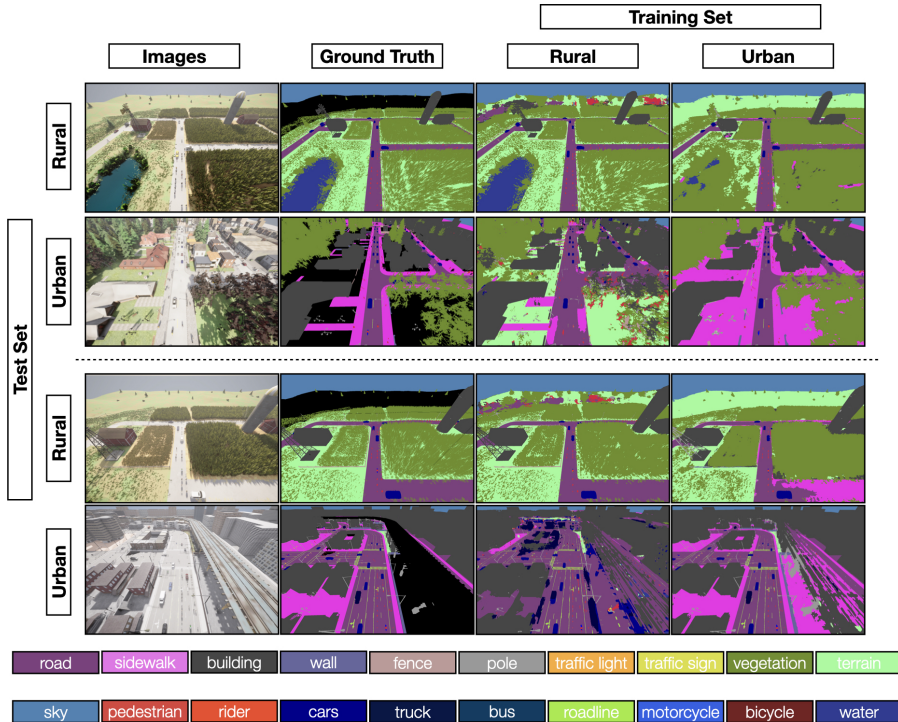


Fig. 18: Semantic Segmentation predictions across rural and urban town variations Semantic segmentation predictions made on held-out SKYSCENES images across rural and urban scenes by a DAFormer [16] model trained on rural and urban scenes respectively. The first two columns indicate the original image and the associated ground truth, column 3 is predictions by model trained on rural scenes subset, column 4 is predictions by models trained on urban scenes subset.

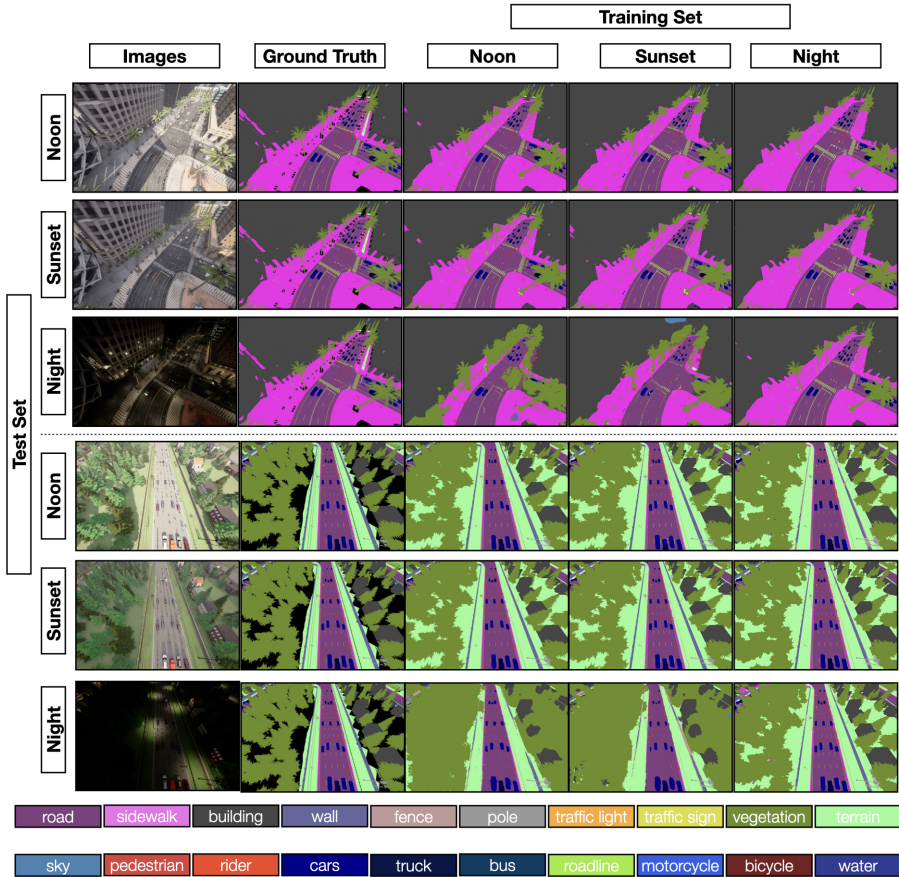


Fig. 19: Semantic Segmentation predictions across different daytime variations Semantic segmentation predictions made on held-out SKYSCENES images across all daytime variations by a DAFormer [16] model trained on select daytime variations. The first two columns indicate the original image and the associated ground truth, column 3 is predictions by model trained on Noon subset, column 4 is predictions by models trained on Sunset subset and column 5 is predictions by model trained on Night subset.

AEROSCAPES, and ICG DRONE respectively. In Fig. 19 and 18, we show how predictions are impacted by changing SKYSCENES conditions.

E Limitations

Depth of distant objects in SKYSCENES is imperfect, akin to real-world conditions. As evident from Fig. 5 in the paper, depth observations struggle to discern finer details of high-altitude viewpoints. We hypothesize that improvement from depth is helpful only for objects close to the camera or lower altitude viewpoints.

F Future Work

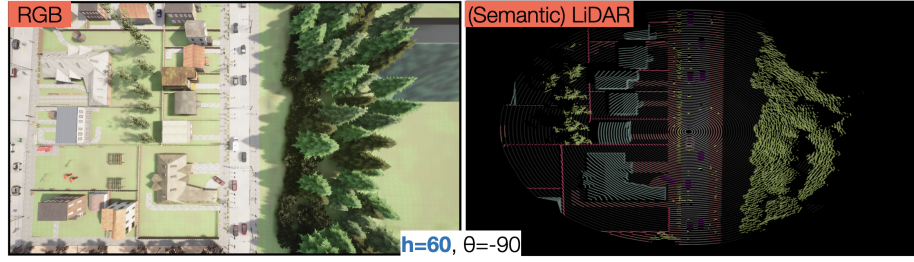


Fig. 20: Demonstrating support for 3D perception tasks in SKYSCENES in future iterations SKYSCENES RGB and corresponding Semantic LiDAR image generated for ($h = 60m$, $\theta = 90^\circ$) and ClearNoon setting.

We plan on updating SKYSCENES with evolving considerations for real-world aerial scene-understanding – improved realism, additional anticipated edge cases – as more and more features are supported in the underlying simulator and provide additional support for 3D perception tasks (see Fig. 20.)